

# **The Role of FMRP in Stalled Ribosomes**

Jewel (Tian-Yi) Li

Neurology and Neurosurgery

McGill University, Montreal, Quebec

April 2024

A thesis submitted to McGill University in partial fulfillment of the requirement of the degree of  
Master of Science

© Jewel Tian-Yi Li 2024

## Table of Contents

<b>Abstract</b>	<b>4</b>
<b>Résumé</b>	<b>5</b>
<b>List of Symbols and Abbreviations</b>	<b>6</b>
<b>Acknowledgements</b>	<b>8</b>
<b>Contribution of Authors:</b>	<b>12</b>
<b>Introduction</b>	<b>14</b>
<i>Importance of Local Protein Synthesis</i>	14
<i>LTP &amp; LTD with Protein Synthesis:</i>	15
<i>Translational Control in Neurons:</i>	16
<i>Characterization of Stalled Ribosomes:</i>	19
<i>Differences in Monosomes, Polysomes and RNA Granules in Neurons:</i>	21
<i>FMRP and Its Many Functions:</i>	23
<b>Materials and Methodology</b>	<b>25</b>
<i>Purification of the RNA Granule-Enriched Fraction</i>	25
<i>Immunoblotting and Quantification of Enrichment</i>	26
<i>Inhibition of Puromycylation by Anisomycin</i>	27
<i>Digestion and Extraction of the Monosomes</i>	28
<i>Linker Ligation</i>	28
<i>RNA Sequence Analysis</i>	29
<b>Results</b>	<b>30</b>
<i>RNA Binding Protein Differences in WT and FMRI-KO RNA Granules</i>	30
<i>Anisomycin and Puromycin Competition Indicates the similarity in WT and FMRI-KO RNA Granules</i>	34
<i>Effects of Digestion and Mg<sup>2+</sup> on the Structure and Ribosomes Protected Fragments in RNA Granules</i>	37
<i>Characterization of the Ribosome Protected Fragments of mRNAs in the WT and FMRI-KO RNA Granules through DEG and GO Analysis</i>	43
<i>Comparison of the Ribosome Protected Fragments of mRNA in the WT and FMRI-KO Analysis to Selected Datasets</i>	46
<i>Peak Analysis on the WT and FMRI-KO RNA Granules</i>	61
<b>Conclusion &amp; Discussion</b>	<b>64</b>
	2



## **Abstract**

Local protein synthesis is a crucial process that maintains essential functions such as synaptic plasticity. A study has demonstrated that a subset of local protein synthesis, such as the ones invoked by mGluR-LTD, is governed by stalled ribosomes -- ribosomes that are paused at elongation. However, how the stalling occurs in neurons is unclear. Previous study has shown that the Fragile X Mental Retardation Protein (FMRP) is highly enriched in RNA granules containing stalled ribosomes (El Fatimy et al., 2016; Anadolu et al., 2023). FMRP, a multi-functional protein, is involved in many neuronal processes, including repression of translation at initiation (Napoli et al., 2008; Santini et al., 2017; Hooshmandi et al., 2023), granule formation (Zhang et al., 2022), and associated with heavy ribosomes resistant to run-off by initiation inhibitor (Cemen et al 2003; Darnell et al 2011). In this study, we attempted to determine if FMRP affected stalled ribosomes containing RNA Granules through investigating the differences between the wild type and FMR1-KO RNA Granules. We examined proteins key to stalled ribosome formation using immunoblotting, the ribosome structure through anisomycin and puromycin competition, and the stall site of these ribosomes on the mRNAs. We found that overall, the loss of FMRP had minor effects on the proteins, structure of the ribosomes and the overall distribution of RPFs but significantly decreased the amount of stalling on mRNAs previously shown to associate with FMRP, suggesting that FMRP regulates stalling of a subset of mRNAs.

## **Résumé**

La synthèse locale des protéines est un processus crucial pour le maintien des fonctions essentielles telles que la plasticité synaptique. Une étude a démontré qu'un sous-ensemble de la synthèse protéique locale, comme celles invoquées par mGluR-LTD, est régie par des ribosomes bloqués - ces mêmes ribosomes qui sont en pause lors de l'élongation. Cependant, la manière dont le blocage se produit dans les neurones n'est pas tout à fait évidente. En effet, Une étude antérieure faite par notre laboratoire démontre que la protéine de retard mental Fragile X (FMRP) est hautement enrichie en granules d'ARN contenant des ribosomes bloqués (El Fatimy et al., 2016 ; Anadolu et al., 2023). La FMRP, une protéine multifonctionnelle-impliquée dans de nombreux processus neuronaux, notamment la répression de la traduction à l'initiation (Napoli et al., 2008 ; Santini et al., 2017 ; Hooshmandi et al., 2023), la formation de granules (Zhang et al., 2022), et associée à des ribosomes lourds résistants au ruissellement par inhibiteur d'initiation (Cemen et al 2003 ; Darnell et al 2011). Dans notre étude, nous avons tenté de déterminer si la protéine FMRP affecte les ribosomes bloqués contenant des granules d'ARN en étudiant les différences entre les granules d'ARN de type sauvage et FMR1-KO. Nous avons pu examiner les protéines essentielles au blocage de la formation des ribosomes en utilisant une technique biochimique appelée Immunoblot, en observant la structure des ribosomes par compétition entre l'anisomycine et la puromycine, ainsi que le site de blocage de ces ribosomes sur les ARN messagers. A travers cette étude, nous avons constaté une perte de protéine FMRP en supplément d'effets mineurs sur les protéines, la structure des ribosomes et la distribution globale des RPF, cependant, nous avons aussi constaté une diminution significative de la quantité de blocage des ARN messagers précédemment associés à la FMRP, ce qui suggère que FMRP a une fonction régulatrice dans les d'ARN.

## **List of Symbols and Abbreviations**

40S – Small Ribosomal Subunit in eukaryotes

60S – Large Ribosomal Subunit in eukaryotes

80S – Complete Ribosome in eukaryotes)

4E-BP – Eukaryotic Translation Initiation Factor 4E (eIF4E)– Binding Protein

AMPA – L- $\alpha$ -amino-3-hydroxy-5-methyl-4-isoxazolepropionic Acid Receptor

Arc – Activity-Regulated Cytoskeleton-Associated Protein

BDNF – Brain-derived neurotrophic factor

CamKII – Calmodulin-Dependent Protein Kinase II

Cryo-EM – Cryo-Electron Microscopy

CREB – cAMP Response Element-Binding Protein

CYFIP1— Cytoplasmic FMR1 Interacting Protein 1

DHPG – Dihydroxyphenylglycine

eIF2 – eukaryotic Initiation Factor 2

eIF2 $\alpha$  – eukaryotic Initiation Factor 2  $\alpha$

eIF2b – eukaryotic Initiation Factor 2b

eIF4E – eukaryotic Initiation Factor 4E

eIF4G – eukaryotic Initiation Factor 4G

eEF1 $\alpha$  – eukaryotic Elongation Factor 1 $\alpha$

eEF2 – eukaryotic Elongation Factor 2

eEF2K – eukaryotic Elongation Factor 2 Kinase

FMR1 – Fragile X Messenger Ribonucleoprotein 1

FMRP – Fragile X Mental Retardation Protein

FMR1-KO – Fragile X Messenger Ribonucleoprotein 1 – Knock-Out

FXS – Fragile X Syndrome

GABA – Gamma-Aminobutyric Acid

GDP – Guanosine diphosphate

GFP – Green Florescent Protein

GTP – Guanosine-5'-triphosphate

GluA1 – Glutamate A1

HITS-Clip – High-Throughput Sequencing of RNA Isolated by Crosslinking Immunoprecipitation

HHT -- Homoharringtonin

LTD – Long term depression

LTP – Long term potentiation

Map1b – Microtubule Associated Protein 1b

Met-tRNA—methionyl-tRNA

mGluR – metabotropic Glutamate Receptor

mGluR-LTD -- metabotropic Glutamate Receptor dependent Long Term Depression

mRNA – Messenger RNA

mTOR – Mammalian Target of Rapamycin

NMD – Nonesense Mediated Decay

PatA – Pateamine A

PKM $\zeta$  – Protein Kinase M $\zeta$

RBP – RNA Binding Protein

RPF – Ribosome Protected Fragments

RNAi – RNA interference

RISC complex – RNA-Induced Silencing Complex

S6K – 40S Ribosomal S6 Kinase

Stau2 – Double stranded RNA-binding protein Staufen homolog2

snoRNA – small nucleolar RNAs

tRNA – transporter RNA

UPF1 – Up-Frameshift Protein 1

## **List of Figures**

Figure 1: Characterization of RNA Binding Proteins in WT and FMR1-KO RNA Granules (33)

Figure 2: Anisomycin and Puromycin Competition in WT and FMR1-KO RG (36)

Figure 3: High Nuclease Treatment Results on Ribosome Protected Fragments (39)

Figure 4: Cryo-EM and GO Analysis of the Impact of High Mg<sup>2+</sup> on RNA Granules (42)

Figure 5: GO Analysis of WT and FMR1-KO Analysis in Abundance, Enrichment and Occupancy (45)

Figure 6: Correlation Analysis to RPFs from Ribosomes Resistant to Run-off and FMRP-Clipped (48)

Figure 7: Correlation Analysis of the Fold Change between WT and FMR1-KO to RPFs from Ribosomes Resistant to Run-off and FMRP-Clipped (49)

Figure 8: Correlation Analysis to mRNAs Regulated by Initiation and Elongation (52)

Figure 9: Correlation Analysis of the Fold Change between WT and FMR1-KO to mRNAs Regulated by Initiation and Elongation (53)

Figure 10: Correlation Analysis to mRNAs translated by Monosome, Polysome and Secretory Proteins (55)

Figure 11: Correlation Analysis of the Fold Change between WT and FMR1-KO to mRNAs translated by Monosome, Polysome and Secretory Proteins (56)

Figure 12: Correlation Analysis to Other Datasets of Interest (59)

Figure 13: Correlation Analysis of the Fold Change between WT and FMR1-KO to Other Datasets of Interest (60)

Figure 14: Peak Analysis of WT and FMR1-KO RG (63)

## **Acknowledgements**

I extend my sincerest thanks to my supervisor Dr. Wayne Sossin, who never fails to amaze me with his knowledge of the current literature and strength in exploring the uncharted territories in science. Even though the revision process is monotonous and borderline torturous, you remained patient in guiding me through the process. Thank you for your teachings in science and in writing. Thank you for your encouragement to pursue different routes in science and more. I will miss the many enthusiastic talks you had with me about the ideas on all the conflicting results.

I would also like to express my heartfelt appreciation to my thesis committee members, Dr. Heidi McBride and Dr. Keith Murai, for their constructive feedback, challenging questions and invaluable insights. Your approachability made the review process a lot less intimidating. I truly appreciate your willingness to meet with me about learning new methods and career trajectory.

My special thanks go to Dr. Mina Anadolu, who taught me everything about this project and in the time I most needed, pushed me forward in writing my thesis. I will forever remember how you started the movement to update your funding within a month. You are the living proof that thoughts can become action.

My gratitude extends to the faculty and staff of the IPN department at McGill University, especially the faculties that participate in research discussions. My special thanks go to Elizabeth Hua from the Fournier Lab and David Foubert from the Ruthazer lab, your dedication in holding research discussions and the offshoot events made the community a better place. Special thanks to Dr. Zhao who brought the best beer and chips to the research discussion. It was remarkable.

To my peers and colleagues, who have shared this journey with me-- Edna Amoah, Elizabeth Hua, Kali Heale, Aliyah Zaman, Sienna Drake, David Foubert, Anna Kim, Aryan Noor and Isabella Lara-- you guys made my Master's journey wonderful and memorable. Thank you for your encouragement, boundless support, and the many little snacks I received, which kept me mentally going. I will always remember the whiteboard in front of the computer room with impressive illustrations and fun questions.

To Xiaotang Fan, thank you for always being here. Your warm encouragement and our small talk always brightened my day. To CongYao, thank you for figuring out the western blot apparatus issue with me. To Linda Michel, thank you for organizing the confusing fundings and processing my travel reimbursement. It looked tedious and your perseverance astounds me. Thank you to Ivannia Murillo who helped me with the mice. Without the mice, there will be no project.

To my parents and Dumpling, I know you both do not read English... so I guess that's it! Just kidding. Thank you for your dedication to my education. I have the opportunity that few have, because of your sacrifice. I love you both. Thanks to Dumpling for being inherently cute. It was a great comfort. My special thanks to my little brother, Owen. Your strength in this harsh economy is inspiring. I am so proud of you. An additional thank you since you will need to translate this.

Thank you to CIHR and Azreli Foundation for providing the funds for this project. I extend my gratitude to the Ortega Lab, JingYu Sun and Dr. Joaquin Ortega for their insights and work on the stalled ribosomes. I also thank Dr. Senthil Kumar Duraikannu Kailasam for

processing my data and sitting with me to figure out the complicated sequencing results. In addition, I thank Dr. Mehdi Amiri who provided Oligos and taught me ribosomal profiling.

Lastly, I extend my appreciation to Chenghao Liu. I feel incredibly lucky to have met you here. You never stop believing in me or encouraging me. We can talk about anything, including AI, 萬曆十五年, Henry Kissinger's kill count, etc. Your support and love made this journey magical. I hope we do not break up, or this paragraph will become hilarious.

### **Contribution of Authors:**

**Li J T-Y** Wrote the thesis

**Sossin WS** Reviewed and edited the thesis

Results:

**Li J T-Y** Contributed figures 1, 2, 3a, 4b, 5, 6, 7, 8, 9, 10, 11, 12, 13, 14. Wet Lab: Dissected the rat and mouse brains for the experiments, prepared the RNA Granule and Ribosomal Clusters, characterized the sucrose gradient fractions using Coomassie, identified RNA Granule protein using western blot, performed and analyzed anisomycin and puromycin competition experiments, extracted RNA from whole brain lysate for sequencing, performed parts of the ribosome profiling process such as digestion of the ribosomes, gel imaging, RNA extraction, linker ligation, and parts of RT-PCR. Bioinformatics: identified non-coding RNAs and coding RNAs, performed DEG Analysis, GO analysis and compared the RPFs to selected dataset.

**Amiri M** Taught me the ribosomal profiling technique, executed parts of the profiling process, such as imaging, gel excision, rRNA depletion, and RT PCR, provided the oligos for the technique.

**Kailasam SK** Contributed to figures 3b, 3c, 3d, 3e. Processed the raw count data, mapped the RPFs to mRNAs, calculated the periodicity, plotting of 3' and 5' overhangs, correlation analysis between biological and experiment replicates, ran DEG analysis, identified coding and non-coding RNAs, identify the peaks, and performed HOMER Analysis.

**Sun J** Contributed to figures 4a. Prepared the EM grid and took EM images for high  $Mg^{2+}$  and low  $Mg^{2+}$  samples in ribosomal clusters.

**Sossin WS** Supervised the project, evaluated bioinformatics results validity in DEG, GO Analysis and HOMER analysis

## **Introduction**

**Importance of Local Protein Synthesis:** Neurons are structurally unique types of cells that have long extended protrusions. For instance, the average hippocampal pyramidal neurites have a length of 13.5mm (Ishizuka et al., 1995), and it has been documented that axonal tips can extend up to a meter away from the cell body (Debanne et al., 2011). In other words, the sites where neurons communicate with each other—synapses-- are distant from the cell body. These sites require protein synthesis to maintain a healthy local proteome. Thus, to combat the challenge of having a faraway nucleus while maintaining healthy local proteome, neurons utilize local protein synthesis. For local protein synthesis to occur, mRNAs along with the translational machinery are transported down to the ends of the neurites. The proteins can then be manufactured close to the synapses during neuronal stimulus. This shortens the response time and grants more control over protein location (Jung et al., 2014). These unique features make local protein synthesis essential to many neuronal functions, such as homeostasis and axonal outgrowth.

Since synapses are distant from the soma, they often have unique local proteomes (Cohen et al, 2013; Dorrbaum et al, 2018) and localized mRNA (Cajigas et al., 2012). Local protein synthesis maintains synapse homeostasis. In the hippocampus, blocking action potentials activates local protein synthesis dependent insertion of GluA1 AMPARs to stabilize the synaptic functions in the hippocampus and compensate for the sudden loss in action potential (Sutton et al., 2006). In addition to local protein synthesis's role in homeostasis, local protein synthesis also participates in neuronal outgrowth and axon guidance. A prominent example is Netrin-1. Netrin-1 is an axon branching factor and a dendritic and axon guidance cue (Serafini et al., 1994). It promotes axon branching through the activation of initiation factors (Campbell & Holt, 2001), which lead to locally synthesized ribosomal protein S4 in retinal ganglia cells (Shigeoka et al., 2019). These

locally synthesized ribosomal proteins are then incorporated to aid axon branching (Shigeoka et al., 2019). Besides maintaining local homeostasis and axonal outgrowth, local protein synthesis also plays crucial roles in synaptic plasticity.

**LTP & LTD with Protein Synthesis:** Synaptic plasticity describes the modulation of strength between neurons. One form of the strengthening of the synaptic connection by stimulation is termed long term potentiation (LTP). There are many pathways for LTP within various brain regions. One of them is NMDAR dependent LTP, where depolarization leads to the removal of the  $Mg^{2+}$  ion in the pore of NMDA receptors, allowing  $Na^+$ ,  $K^+$  and most importantly  $Ca^{2+}$  to flow in. In early-LTP,  $Ca^{2+}$  activates CAMKII and leads to the synaptic recruitment of AMPAR, which stabilizes the post-synaptic density and results in the strengthening of synapses. Late-LTP induces CREB phosphorylation. This triggers many transcription pathways, which lead to synthesis of many important neuronal factors. This is also the reason late-LTP has been reported to require de novo mRNA synthesis (Baltaci et al., 2019). One factor activated by CREB phosphorylation is Brain-derived neurotrophic factor (BDNF) (Bonnie et al., 1999). Amongst BDNF's many roles, the downstream pathway of BDNF regulates transport of mRNA to dendrites (Bramham & Messaoudi, 2005). Transportation of these mRNA may be crucial for Late-LTP. Activity regulated cytoskeleton associated protein (arc) is one of these mRNAs that are transported through BDNF activation. LTP can be impaired when arc is degraded (Guzowski et al., 2000). Besides arc, the mTOR pathway is also activated by effectors downstream of BDNF (Takei et al., 2004). mTOR, mammalian target of rapamycin, regulates translational factors (Takei et al., 2004; Hoeffler & Klann, 2010). When mTOR is inhibited by rapamycin, it reduces late-LTP in hippocampus (Tang et al., 2002). Another important effector down stream of BDNF that is synthesized locally is PKM  $\zeta$  (Mei et al., 2011). PKM $\zeta$  maintains late-LTP by preventing AMPAR endocytosis in CA1

hippocampal neurons (Yao, 2008). It has also been documented that PKM $\zeta$  mRNA is transported to the synapse and is transcribed locally downstream of LTP signaling pathway (Muslimov, 2004). Together, these studies show that local protein synthesis may play a role in late-LTP.

Long-term depression (LTD) is a form of synaptic plasticity that describes the weakening of synaptic strength. mGluR-dependent-LTD is one of the many forms of LTD. Protein synthesis is crucial to mGluR-LTD. When protein synthesis is inhibited, mGluR-LTD is lost (Huber et al., 2000). In addition, mTOR may also be involved in LTD through protein translation. When mTOR is inhibited by rapamycin in hippocampus, mGluR-LTD is abolished (Hou & Klann, 2004). Molecularly, many locally translated proteins are crucial to mGluR-LTD. In hippocampus, arc mRNA, which is rapidly sent to dendrites after synthesis (Steward & Worley, 2001), are translated in response to mGluR and stimulates AMPAR endocytosis (Waung et al., 2008). When arc is knocked down, endocytosis of AMPAR is disrupted, resulting LTD inhibition (Waung et al., 2008). Similarly, microtubule associated protein 1b (MAP1b) is also regulated by mGluR activity (Davidkova & Carroll, 2007). When MAP1b is reduced in dendrites, AMPAR endocytosis, too, is disrupted (Davidkova & Carroll, 2007), indicating that local protein synthesis of MAP1b is important to mGluR-LTD. All these examples showed the essential function of protein synthesis to mGluR-LTD. Overall, local protein synthesis heavily supports synaptic plasticity in late-LTP and mGluR-LTD.

**Translational Control in Neurons:** Local Protein translation requires repression of translation during transport, which makes translational control crucial. Besides translational control via RNA Binding Proteins (RBPs), translation factors are heavily regulated in neurons. Translation is divided into three phases: initiation, elongation, and termination. Translational control at initiation, perhaps, is the most well studied for local protein synthesis. Initiation itself can be divided into

three parts: 1) creation of 43S ribosomal preinitiation complex, 2) the binding of preinitiation complex to the mRNA, and 3) the formation of 80S ribosomal complex (Buffington et al., 2014). All these steps are heavily regulated by translation initiation factors, including the  $\alpha$  subunit of eIF2 (eIF2 $\alpha$ ). eIF2 $\alpha$  associates with the Initiator Met-tRNA, and in its GTP-bound form begins the formation of 43S ribosomal preinitiation complex (Costa-Mattioli et al., 2009; Buffington et al., 2014). When eIF2 $\alpha$  is phosphorylated, eIF2b, eIF2's guanine nucleotide exchange factor, can no longer convert the GDP associated to eIF2 into GTP, leading to the loss of eIF2's ability to form preinitiation complex and reduce translation. Neuronal activity, such as reduced GABAergic transmission (Zhu et al., 2011), can control phosphorylation of eIF2 $\alpha$  and alter translation. Translation control at initiation is also crucial for learning and memory; for example, when kinases that phosphorylate eIF2 $\alpha$  are decreased, memory improves (Costa-Mattioli et al., 2005; Zhu et al., 2011). Another significant regulator is the eIF4E binding proteins (4E-BP). 4E-BP, like its name, binds to eIF4E and prevents eIF4E from binding to eIF4G. Without the eIF4E-eIF4G complex, the pre-initiation complex 43S ribosomes will not identify the 5'Cap of the mRNA, leading to inhibition of initiation. Like eIF2 $\alpha$ , 4E-BP, too, is regulated by neuronal activity through phosphorylation. For instance, mTOR, which can be triggered by L-LTP (Takei et al., 2004; Carroll et al., 2004; Hoeffler & Klann, 2010) and LTD (Hou & Klann, 2004), results in the phosphorylation of 4E-BP. When 4E-BP is knocked out in mice, spatial memory is impaired (Banko et al., 2005). Overall, translational control at initiation is crucial for synaptic plasticity.

On the other hand, translational control through elongation is much less studied. During elongation, eEF1 $\alpha$  brings in the tRNA to the A site of the ribosome. If the mRNA matches with the tRNA, the ribosome will catalyze the peptide joining. This leads to a rotation of the large and small ribosomal subunit in respect of each other. The A site tRNA stays bound to the A site of the

small ribosomal subunit, but the tRNA ends up in the P site of the large ribosomal subunit. This is referred to as the A/P tRNA. Similarly, the P site tRNA remains associated to the P site of the small ribosomal subunit but relocates to the E site of the large subunit. This is termed the P/E tRNA. The rotated ribosome is named the hybrid state. Finally, eEF2 comes in, translocate the mRNA along with the small subunit, and rotated the ribosomes back to their original state to allow translation to proceed (Dever et al., 2018). Neuronal activity regulates elongation through eEF2 phosphorylation and dephosphorylation. For example, NMDAR activation can lead to eEF2 phosphorylation (Sutton et al., 2007). Another pathway which regulates eEF2 is the mTOR pathway. Besides eIF2 $\alpha$  phosphorylation, mTOR also triggers the phosphorylation of S6 Kinase (S6K) to regulate protein synthesis. S6K phosphorylates eEF2 Kinase (eEF2K), which decreases eEF2K activity and allows eEF2 to be dephosphorylated and proceed with translation (Wang et al., 2001). Phosphorylation of eEF2 causes an inhibition of its association to ribosomes. Thus, phosphorylation of eEF2 should inhibit or slow elongation, but for unknown reasons, eEF2 phosphorylation increases selective mRNA translation in neurons (Park et al., 2008). Like translational control in initiation, translational control in elongation is crucial for synaptic plasticity. Irregularity in eEF2K may cause neuronal disease. For instance, studies had shown Alzheimer's disease patients have irregularities in the amount of eEF2K in their brain tissues, and reduction of the increased eEF2 improves long term memory and synaptic plasticity in mouse model of autism (Ma, 2021). Furthermore, the occurrence of mGluR-LTD seems to be primarily reliant on translation control at elongation. A study found that mGluR-LTD is inhibited by elongation inhibitors, but not by initiation inhibitors (Graber et al., 2013). Other studies note the effect of elongation inhibition on crucial neuronal protein. Inhibition of eEF2 phosphorylation reduces the mGluR-LTD induced protein synthesis of MAP1b (Davidkova & Carroll, 2007, Graber et al.,

2013) and arc (Park et al., 2008). In addition, phosphorylation of eEF2 seems to be able to regulate dormant ribosomes, ribosomes that do not contain mRNA or tRNAs. A study demonstrated that eEF2-phosphorylation leads to the stabilization of inactive ribosomes in p-bodies, a form of liquid-liquid separated granules (Smith et al., 2021). Together, these studies demonstrated the crucial effects translational control at elongation is on protein synthesis. Besides translational control through elongation factor, a study has found that mGluR-LTD induced protein synthesis seems to rely on the reactivation of stalled ribosomes, ribosomes that are paused at elongation (Graber et al., 2013).

**Characterization of Stalled Ribosomes:** In neurons there are ribosomes that are repressed at elongation (Graber et al., 2013). In the study, puromycin is used to label nascent peptides on the ribosomes. This method is called puromycylation. Puromycin mimics the upper half of the tRNA and is covalently attached to the nascent peptide by the ribosome. Normally, when initiation inhibitors are added to the solution, the assembly of new ribosomes on the mRNA is blocked, and the targets of puromycin decrease as time passes since the already translating ribosomes will eventually finish their job, and fewer nascent peptides remain on ribosomes. In other words, the ribosomes are run-off. However, in neuronal hippocampal cultures, the puromycin signal between the condition with and without the presence of initiation inhibitors such as Patamine A (PatA) and homoharringtonin (HHT), does not differ from each other. Thus, most ribosomes are stalled. In contrast, in a normal cell line, such as the HEK-293 cells, initiation inhibitors strongly reduce puromycylation. This indicated that these stalled ribosomes are unique to neurons. The study located these stalled ribosomes within the puncta like structure in hippocampal neurites after initiation run-off when performing puromycylation (Graber et al., 2013). These puncta colocalizes with ribosomal mRNA and other granule markers (Graber et al, 2013). This suggests that the

ribosomes that are stalled at elongation are in these RNA Granules. Moreover, the study also reveals that these stalled ribosomes are necessary and sufficient in inducing mGluR-LTD. When dihydroxyphenylglycine (DHPG) is administered to induce mGluR-LTD, the stalled ribosomes diminish, even after runoff using initiation inhibitors (Graber et al., 2013). DHPG also induces an increase in protein synthesis of MAP1b in the presence of an initiation inhibitor. Lastly, inhibiting initiation dependent translation with the initiation inhibitor, HHT, does not affect mGluR-LTD. These experiments indicate that mGluR-LTD relies on initiation independent translation that is likely from the reactivation of these stalled ribosomes.

Further studies using puromycin demonstrated the singularity of stalled ribosomes in neurons. As stated, in normal cell types, puromycin diffuses away despite the presence or absence of elongation inhibitors (Aviner, 2020; Hobson et al., 2020; Enam et al., 2020). However, puromycin is retained in stalled neuronal ribosomes (Langille et al., 2019; Anadolu et al., 2024). A study has utilized this technique to show that in neuronal processes, the SunTag signal does not vanish when puromycin is added regardless of the presence of elongation inhibitor. During the SunTag Assay, artificial mRNA is constructed that when translated into nascent peptide chain, contains binding site for GFP. Thus, GFP are recruited to the extending nascent peptide chain and allows translation to be observed in real time (Wu et al., 2016). In this study, a significant amount of GFP signals remain even after puromycin is added to the solution for 12 minutes (Langille et al., 2019). In addition, CryoEM of puromycylated stalled ribosomes from the RNA Granules illustrates how the puromycin stays attached to the ribosomes despite the loss of tRNA (Anadolu et al., 2024). This indicates that stalled ribosomes in neurons function differently than normal ribosomes.

Distinct stalled ribosomes have been identified to be present in RNA granules (Anadolu et al., 2023). When analyzing the ribosomes in RNA granules enriched from whole brain homogenates with Cryo-EM, it is found that 85% of the ribosomes are in the hybrid state during elongation (Anadolu et al., 2023). However, the question behind how stalling in ribosomes occurs remains ambiguous. Previously, it was shown that UPF1, and Stau-2 are important for stalling to occur (Graber et al., 2017). When using RNAi to knock down UPF1, the number of puromycylated puncta and the DHPG-induced protein synthesis is lost. Similarly, when knocking down Stau2, the puromycylated puncta and the transportation of MAP1b RNA decreases. Though the necessities of Stau2 and UPF1 for stalled ribosomes are confirmed, how Stau2 and UPF1 aid in the stalling of the ribosomes is unknown. Another protein observed to colocalize with puromycylated puncta is Fragile X Mental Retardation Protein (FMRP)(Graber et al., 2013). FMRP is highly enriched in RNA Granules (Anadolu et al., 2022). In addition, the ribosomal footprints (RPF) of the ribosomes in these RNA Granules are stalled at sequences enriched in motifs previously associated with FMRP Clip data (Ascano et al, 2012; Anderson et al., 2016; Anadolu et al., 2023). All of these indicate FMRP to be potentially important to the stalling in neuronal ribosomes.

**Differences in Monosomes, Polysomes and RNA Granules in Neurons:** There are two forms of assembled ribosomes in a cell -- polysomes and monosomes. Polysomes are described as two or more ribosomes attached to one individual mRNA. Monosomes consist of one single mRNA that is bound to one individual ribosome. Monosomes are generally believed to be non-translating due to the high percentage of empty ribosomes when sequencing the lighter fraction of a sucrose gradient (Krichevsky & Kosik et al., 2001; Kelen et al., 2009; Liu & Qian, 2016; Masek et al., 2020). Yet, the notion that a monosome does not contain translating ribosomes is changing. A recent study had shown the translating monosome from yeast may be crucial in regulating the

negative feedback loop of protein production and nonsense mediated decay (NMD) (Heyes & Moore, 2016). More importantly, another study has indicated monosomes are the translating machinery for local protein synthesis in neurons since monosomes are enriched in neuronal processes (Biever et al., 2020). In addition, the study also demonstrated that monosomes are associated to synapse related mRNA and these selected mRNAs are highly abundant in pre and post synapses (Biever et al., 2020). Thus, monosomes may be the main translational machinery for local protein synthesis.

Polysomes have been recognized as the main translating machinery in cells. Polysomes are enriched in the heavy fraction of the sucrose gradients during high centrifugation (Warner et al., 1963; Risebrough et al., 1962; Warner & Knopf et al., 2002). Though in neurons, polysomes are essential to translation (Ekholm & Hyden, 1965; Wenzel et al., 1975; Bagni et al., 2000; Biever et al., 2020), some studies have shown that a portion of the polysomes extracted from neurons are insensitive to translational inhibitor puromycin (Stefani et al., 2004; Darnell et al., 2011). Later studies also find a portion of polysomes are resistant to other initiation inhibitors, such as homoharringtonine (HHT) (Shah et al., 2020; Popper et al., 2024). These studies indicated that there are stalled neuronal ribosomes in the polysome fraction. Yet, it is unclear whether these are stalled polysomes or stalled monosomes that are packaged into ribosomal clusters.

There are many similarities between RNA Granules and polysomes. However, RNA granules are denser than polysomes and are found in the pellet of these sucrose gradients while polysomes (El Fatimy et al., 2016; Anadolu et al., 2023) remain in the lighter fractions. While some differences in the organization of the ribosome clusters between the RNA Granules and polysome fractions have been observed (El Fatimy et al., 2016; Kipper et al., 2020), this is not consistent across studies (Anadolu et al., 2023). Similarly, when looking at the the ability for

nuclease to cleave unprotected ribosomes into monosomes, studies also show variability. One study shows RNA Granules are resistant to nuclease digestion while polysomes are sensitive (El Fatimy et al, 2016). Others show nuclease affects RNA Granules (Kipper et al., 2020; Anadolu et al., 2023), although higher concentrations of nuclease may be required. Thus, structurally, ribosomes from polysome fraction and RNA Granules are comparable to each other. However, in RNA binding protein, there is a key difference between the enrichment of FMRP in RNA Granules compared to polysomes (El Fatimy et al., 2016; Anadolu et al., 2023).

**FMRP and Its Many Functions:** Fragile X Syndrome (FXS) is the largest single leading genetic cause of autism-spectrum disorder (Richter & Zhou, 2021). FXS affects 1 in 4000 males and 1 in 7000 females. The gender discrepancy of the disease is due to FMR1 residing on the X chromosomes (Richter & Zhou, 2021). Molecularly, FXS is caused by CGG expansion in FMR1, which leads to loss of the FMRP. Naturally, FMRP becomes a prime target for neuronal study, which contributes to the extensiveness of related research, such as FMRP's association to stress granule (Cheever & Ceman, 2009; Lai et al.; 2020, Richter & Zhao, 2021), association to the RISC complex (Cheever & Ceman, 2009; Lai et al., 2020; Richter & Zhao, 2021), and the ability to directly activate ion channels (Gross et al., 2011; Ferron, 2016; Deng & Klyachko, 2021; Richter & Zhao, 2021). However, for our study, we will focus on its interaction with local protein translation, translational repression, and mGluR-LTD.

FMRP has been documented to affect local protein synthesis and translational control. The loss of FMRP leads to irregularities in the local proteome. When FMRP is knocked out, the dendritic level of arc in hippocampus increases, but mGluR-induced arc synthesis is absent (Niere et al., 2012). Similarly, MAP1b also has been shown to increase in the hippocampus of FMRP knockout mice (Huber, 2002). FMRP can repress translation through initiation. FMRP binds to

cytoplasmic FMRP-interacting protein 1 (CYFIP1), and the FMRP-CYFIP1 interacts with eIF4E, which sequester translation (Napoli et al., 2008). An example of FMRP halting translation through CYFIP1 is when CYFIP1 is inhibited through siRNAs, MAP1b increases (Napoli et al., 2008). The loss of FMRP also has profound effects on initiation. It has been reported that FMRP-KO mice seem to be rescued by altering initiation pathway as eIF2 $\alpha$  phosphorylation (Hooshmandi et al., 2023), or reducing eIF4e-eIF4G interaction (Santini et al., 2017). Alternatively, FMRP also may sequester translation formation of liquid-liquid phase separated granules. FMRP contains a RGG low complexity domain, which leads to spontaneous formation of liquid-liquid phase separated granules when binding to mRNA (Tsang et al., 2019; Zhang et al., 2022). Together, these studies showed the many effects of FMRP on local protein translation and translation control.

The loss of FMRP enhances mGluR-LTD and makes it independent of protein synthesis (Hou et al., 2006; Nosyreva and Huber, 2006). One of the ways is through FMRP's binding partner CYFIP1. mGluR-stimulated dissociation of the CYFIP1-eIF4E complex, which effectively ends translational repression (Napoli et al., 2008). Interestingly, even though mGluR-LTD enhances translation, the mGluR-LTD synthesis of MAP1b seems to be abolished in FMRP-KO mouse (Hou et al., 2006). On the other hand, mGluR activation is also essential for the regulation of FMRP levels. For example, the activation of group 1 mGluRs leads to the dephosphorylation of FMRP and results in the degradation of FMRP (Narayanan et al., 2007; Nalavadi et al., 2012). Additionally, the activation of mGluR5 triggers the sumoylation of FMRP which results in its dissociation from RNA Granules (Khayachi et al., 2018). The lowered level of FMRP through two post translational modification of mGluR stimulus effectively lower its association to mRNA and halting the repression. The relevance of FMRP in local protein synthesis, translational repression and mGluR-LTD made its role for our stalled ribosomes even more intriguing.

FMRP also has been implicated in the stalling of the ribosomes. Several studies have shown FMRP remains colocalized with the ribosomes after run-off assays using initiation inhibitors (Ceman et al., 2003; Darnell et al., 2011). Besides, loss of FMRP has been shown to enhance mGluR-LTD (Hou et al 2006), and mGluR-LTD is a key pathway for stalled polysomes reactivation (Graber et al., 2013). Most importantly, FMRP is enriched in stalled ribosomes containing RNA Granule (Graber et al., 2013, El Fatimy et al., 2016; Anadolu et al., 2023). All this evidence shows FMRP is related to stalled ribosomes. Yet, the many functions of FMRP make it difficult to discern the relevance of FMRP to stalled ribosomes. Thus, the question for this study is to identify if FMRP is crucial for stalled ribosome formation. We propose that FMRP is important for selecting a subset of mRNAs that are present in stalled polysomes rather than determining the formation of stalled polysomes. To test this, we examined the differences between the proteins, structure of the ribosomes, mRNAs and the stalling sites of the ribosomes in RNA Granules extracted from WT and FMR1-KO mouse.

## **Materials and Methodology**

### **Purification of the RNA Granule-Enriched Fraction**

All preparations used brains that were flash frozen using liquid nitrogen or dry ice ethanol bath. Either 5 postnatal day sprague dawley rat brains or 10 whole brains from postnatal day 5 (P5) C57BL/6 mouse and FMR1-KO mouse from Charles Rivers Laboratory were dissected. Samples were homogenized in either the previous RNA Granule Buffer (20 mM Tris-HCl pH 7.4 (catalog #BP152-1, Thermo Fisher Scientific), 150 mM NaCl (catalog # BP358-212, Thermo Fisher Scientific), 2.5 mM MgCl<sub>2</sub> (catalog# M33-500, Thermo Fisher Scientific)) or high Mg<sup>2+</sup> RNA

Granule Buffer (20 mM Tris-HCl pH 7.4, 150 mM NaCl, 10 mM MgCl<sub>2</sub>). These buffers were supplemented with 1mM DTT (catalog #D9163, Sigma-Aldrich), and 1mM EGTA (catalog # E8145 Sigma-Aldrich) for homogenization. The homogenate was centrifuged 15min in a Thermo Fisher Scientific T865 fixed-angle rotor at 6117 xg at 4°C to separate debris, such as lipid and extracellular matrix, from the ribosomes. A small portion of supernatant was collected as the starter material. The rest were clarified with 1% iGEPAL CA-630 (catalog #04693132001, Roche) for 5 min at 4°C. Sucrose solution was produced by suspending sucrose (catalog #8550, Calbiochem) with RNA Granules buffer. The samples were loaded onto a 60% sucrose pad in a Sorvall 36 ml tube (Kendro, catalog #3141, Thermo Fisher Scientific) and centrifuged at 56,660 x g for two hours in AH-629 swing-bucket rotor to retrieve the polyribosomes. The polyribosome was resuspended in RNA Granule buffer then reloaded onto 15%-60% sucrose gradient and centrifuged at 56,660 xg for 45 min to separate the ribosomes into monosomes, ribosomal clusters and RNA Granule. Each fraction was 3.5 ml and collected from the top. We retrieved Ribosomes Clusters from fraction 5 and 6, RNA Granules from the pellet.

### **Immunoblotting and Quantification of Enrichment**

For Immunoblotting, the RG and RC were ethanol precipitated and resuspended with 1x sample buffer and Granule buffer. The samples were loaded onto 10%, 12% or 15% acrylamide gel according to the observing protein sizes. The gel was either stained with Coomassie Brilliant Blue to look at the protein distribution or transferred onto a 0.45um nitrocellulose membrane (catalog #1620115, Bio-Rad) for immunoblotting. The transferred membranes were stained with Ponceau and imaged. Then, the membranes were blocked with 5% BSA (catalog # A9647, Sigma Aldrich) in Tris-buffered saline with Tween before incubation with primary antibodies- rabbit anti-s6 (1:10,000) (catalog #2217, Cell Signaling Technology), rabbit anti-FMRP

(1:500)(catalog #4317, Cell Signaling Technology), rabbit anti-UPF1 (1:10,000)(catalog #ab133564, Abcam), mouse anti-Stau2 (1:1000)(catalog #MM0037-P, MediMabs), anti-eEF2 (1:1000)(catalog #2332S, Cell Signaling Technology), rabbit anti-Pur-alpha (1:1000)(catalog #ab79936, Abcam), and anti-mouse puromycin (1:1000)(catalog #ab2619605, Developmental Studies Hybridoma Bank). Membranes were washed with TBS-T after incubation. HRP-conjugated secondary antibodies such as anti-rabbit HRP (1:10,000)(catalog #31460, Thermo Fisher Scientific) and anti-mouse HRP (1:10,000)(catalog #31430, Thermo Fisher Scientific) were incubated with the membranes for detection. ECL reaction was performed for imaging, and the images were scanned and quantified by ImageJ software. The single band for each protein was selected and normalized against s6 signal intensity to examine the quantity of the proteins for each sample. The enrichment between the RC and RG was calculated by RG divided by RC. A two tailed, unequal variance t-test was performed between the enrichment of WT and FMR1-KO to observe the differences between the two groups. Data was graphed via excel.

### **Inhibition of Puromylation by Anisomycin**

The liver ribosomes were extracted from P5 Sprague Dawley rats livers through the identical method as the RNA Granules, but without the last spin since liver does not contain RNA Granules. All ribosomal fractions used were incubated for 5 min in 1) RNA Granule buffer 2) 100uM puromycin (catalog# P7255, Sigma Aldrich), or 3) 100uM puromycin and 100uM anisomycin (catalog# A9789, Sigma Aldrich). The samples were then ethanol precipitated, immunoblotted and quantified via the method stated above. The percentage of puromycin resistant to anisomycin inhibition were calculated by dividing the differences between 3) and 2) with 2) then multiplying by 100%.

## **Digestion and Extraction of the Monosomes**

The RC WT and FMR1-KO were loaded onto a 60% sucrose pad and centrifuged to concentrate the samples. For normal nuclease treatment groups, 1 $\mu$ l of RNAase I (100U/ $\mu$ l; catalog #AM2294, Thermo Fisher Scientific) was administered to the RC and RG and rotated at 4°C for 30min. Then, 4 $\mu$ l of SuperaseIN (20U/ $\mu$ l; catalog # AM2969, Invitrogen) was added to the solution to halt the reaction. The samples were then loaded onto 15% to 60% sucrose gradient and centrifuged at 56,660 x g for 45 minutes to retrieve the monosomes from fraction 2 and 3. For high nuclease treatment group, RNAase I (10 U/ $\mu$ l, catalog #N6901K, Epicentre) was adjusted to the concentration of RC and RG via the A260 read from the Nanodrop. Every OD from the A260 equaled 6 units. Thus, the RNAse amount per  $\mu$ l equals OD observed from A260 multiplied by 6unit then divide by 10 for the concentration listed by the company. In addition, the samples were incubated at room temperature for 30min instead of 4 °C. Then, 6 $\mu$ l of SuperaseIN were added to halt the reaction. The samples were then spin at 68,000 xg for 3hrs on a Beckman tabletop ultracentrifuge to concentrate the monosomes, which pellets. The RNA of RC and RG was extracted through the trizole chloroform method followed by isopropanol precipitation to concentrate the samples. The samples were loaded onto Urea gel (catalog # EC68852Box, #EC68752Box, #EC62152Box, ThermoFisher) to select for RPF size. Segments between 25b and just above 40b were excised and retrieved to account for the possible longer fragments of the RPFs. The excised gels were frozen for 30 min on ice and then thawed overnight at room temperature. The RNA was extracted again with trizole chloroform extraction.

## **Linker Ligation**

The steps were adopted from Gincly & Ingolia, 2017. The concentration from the RNA footprint was calculated from Agilent small RNA chips. An equal amount of RNAs were calculated and transferred to a new tube for each sample to ensure each sample has a relatively equal amount after pooling. 3 different linkers (NI-810, NI-811, BI-812 (for sequence of the oligonucleotides, please reference Gincly & Ingolia, 2017)) were attached to each of the replicates. The samples were first dephosphorylated with T4PNK linker (catalog # M0351L, NEB), and then pre-adenylated linkers are attached through T4 Rnl2 (catalog # M0351L, NEB). The linked RNA was purified through excision of urea gel between 50bp and 70bp. Samples in the same variables were then pooled together with their gel fragment combined. The RNA was extracted from the gel with the steps stated previously containing all three replicates, followed by Reverse transcription. MyOne Streptavidin C1 DynaBeads (catalog#65001, ThermoFisher) was used for rRNA depletion. Lastly, PCR was performed. The samples were sequenced through the McGill University Genome Center on NovaSeq S1/2 flow cells.

### **RNA Sequence Analysis**

The adaptor sequences were trimmed using Cutadapt version 2.8 (Martin, 2011). The raw counts were obtained using featurecounts version 2.2.0 (Liao et al., 2014). The noncoding mRNA was removed through matching the mouse genes to available coding mRNA online using R-studio. The raw count of the mRNAs was normalized against gene length, total count and divided by one million to obtain RPKM for abundance. Counts lower than 5 were removed. The RG raw count was divided by total mRNA from the according replicates to obtain the RG occupancy, and RC from the according replicate to calculate the RG enrichment. All RC and total mRNA count that equals to 0 was removed. The Differential Expression Gene Analysis was performed via R studio packages in *edgeR* and *limma* package from Bioconductor adapted for RNA-seq

(Robinson et al., 2010). Gene Ontology (GO) enrichment analysis was performed with *clusterprofiler* from *BioManager* (Wu et al., 2021). Comparison to data online was performed via jupyter notebook and graphed by *boxplot* in *matplotlib*. Peaks identifications were done using R package, where RPFs from each library were compiled and selected when the amplitude is higher than 4x average of the mRNA. These sites also need to be present in all replicates. For the peaks to be considered as present across the replicates, the amplitude of the peaks to be within 6nt of each other. HOMER tool (Heinz et al., 2021) was used for motif analysis.

## **Results**

### **RNA Binding Protein Differences in WT and FMR1-KO RNA Granules**

To explore the effects of FMRP on stalled ribosomes, we enriched RNA Granules from sucrose gradient. Stalled ribosomes are found in RNA Granules (Graber et al., 2011). Previous studies had demonstrated neuronal ribosomes can be separated into monosome and polysome fractions in sucrose gradient during high-velocity spin (Krichevsky and Kosik, 2001; Kanai et al., 2004; Aschrafi et al., 2005; Elvira et al., 2006). This preparation was optimized to separate RNA Granules from the denser polysomes (El Fatimy et al., 2016; Anadolu et al., 2023). We utilized this protocol to collect three fractions for comparison of the composition of RNA granules in the mouse brain preparation compared to the rat brain preparation, the starting material, fractions 5/6, and the pellet, which we term RNA granules fraction (RG) (Fig. 1A). Fraction 5/6 is usually referred to as the polysome fraction. However, since there is no evidence if the stalled ribosomes in the polysome fractions are polysomes or monosomes, we refer to it as Ribosomal Clusters (RC) in this study. To examine if the RG enriched from C57BL-6 (WT)

mice are comparable to the ones extracted from rat brain in previous study (Anadolu et al, 2023), we collected all fractions from the sucrose gradient, loaded them on an SDS gel and stained with Coomassie blue. This allowed us to assess if the protein distribution extracted from rat brains and mouse brains are similar during sucrose gradient sedimentation. We found that the trend in protein distribution was similar between rat and WT mice brain, where there were considerable amounts of proteins in both WT mice RG and rat RG (Fig 1B). We further confirmed WT mice RG and rat RG were comparable to each other through immunoblotting key proteins from previous study such as FMRP, eEF2 and Pur-alpha (Anadolu et al., 2023). Like the previous results from rat RG, WT mice RG were enriched in FMRP when comparing to RC and starter fraction, while eEF2 was unobservable in neither the RC nor RG (1C). Though we no longer see a specific enrichment of Pur $\alpha$  in WT RG, it was present in all fractions. This showed that overall WT mice brains RG was proportional to rat RG, and this allowed us to use WT mice to further study stalled ribosomes in RNA Granules.

To analyze the effect of FMRP on RNA Granules, we decided to examine the RG and RC from FMR1 knockout mice (FMR1-KO). FMR1-KO mice is the most common model for studying FMRP's function and Fragile X Syndrome (Richter & Zhao, 2021). The FMR1-KO mice is derived from C57BL/6 mice with the exon 5 of FMR1 interrupted. FMR1-KO mice exhibit behaviors related to FXS behaviors in humans such as delayed eye-blinking, altered social interaction and repetitive behaviors (Bakker et al., 2000). Molecularly, FMR1-KO mice exhibits abnormalities in synaptic plasticity (Zhang et al., 2009). In addition, since the disruption is not caused by CGG expansion and thus does not exhibit CpG island methylation, FMR1-KO mice allows us to inspect the molecular effects of FMRP independently of possible additional effects of this methylation. The RNA Granules were obtained from homogenized FMR1-KO

mice brain, and the control RNA Granules from homogenized C57BL-6 mice brain. We confirmed that FMRP was knocked out (Fig 1C). Next, we compared the level of ribosomes in the RG and the RC (Fig 1D). If FMRP was critical for formation of RNA Granules, there should be fewer ribosomes in the RG compared to the RC without FMRP. Instead, we observed an increase in the relative levels of S6 ribosomes in FMR1-KO through immunoblots (p-value = 0.07) (Fig 1H). For results below, all quantification of RNA binding proteins (RBPs) was normalized to the levels of S6.

To investigate the loss of FMRP on stalled ribosomes, we looked at two key proteins that are essential for stalled ribosomes formation-- UPF1 and Stau2. UPF1 is enriched in RNA Granules (Anadolu et al., 2023) and the disruption of UPF1 causes significant reduction in RNA Granule formation (Graber et al., 2017). Our result showed that WT and FMR1-KO RG were enriched in UPF1 when comparing to RC (Fig 1C, 1E). Furthermore, the enrichment between the two groups was indiscernible (Fig 1I). Previous study also shows the interaction of UPF1 with Stau2 is also crucial for RNA granule formation (Graber et al., 2017). We examined two isoforms, 59kD isoform which is directly linked to the RNA Granule formation (Graber et al., 2017) and 52 kD isoform which is enriched in neurons and associates to ribosomes (Duchaine et al., 2002). Neither isoform was significantly enriched in RG although there was a trend suggesting a possible increase (Fig 1F, 1G). Similarly, there were no differences in enrichment between WT and FMR1-KO (1J, 1K). Overall, the RBPs most associated to RNA Granule formation-UPF1 and Stau2, were statistically indistinguishable between FMR-KO RG and WT RG, suggesting that FMRP does not grossly affect RNA granule composition, other than the loss of FMRP itself.

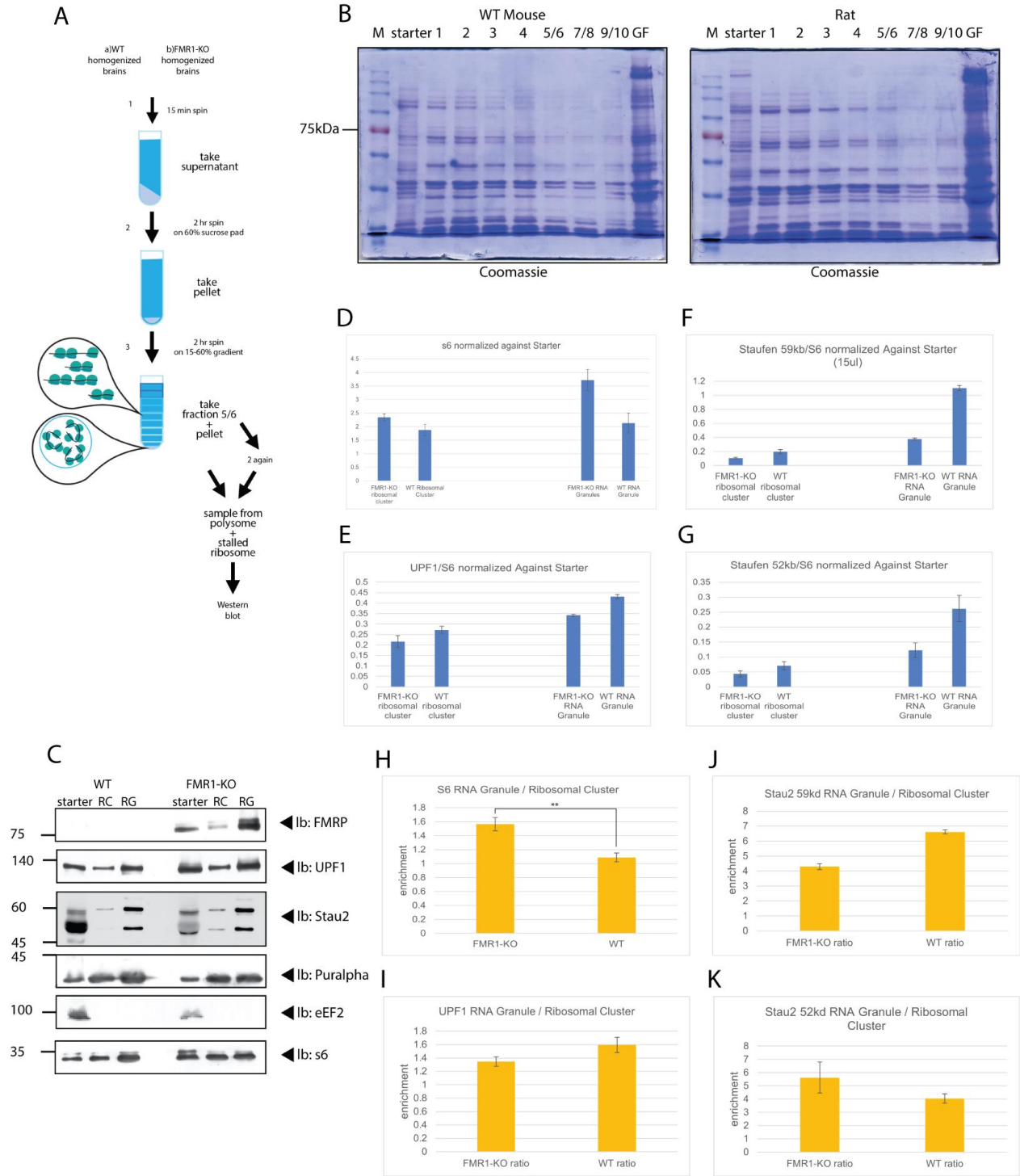


## Figure 1. Characterization of RNA Binding Proteins in WT and FMR1-KO RNA Granules

A) A summary of protocol for isolating the RNA Granules (RG) from C57 and FMR1-KO mouse' who brain homogenate using sucrose gradient fractionation. B) SDS-page stained with Coomassie brilliant blue showing the distribution of proteins from each fraction of the sucrose gradient from WT mouse and rat brains. C) Representative immunoblots for starting materials, ribosomal cluster (RC) from fraction 5/6 of the sucrose gradient and RNA Granules (RG) from the pellet of the sucrose gradient stained for RBPs that are crucial for stalled ribosomes or related to stalling. D-F) The Quantification of s6 (N = 6), UPF1 (N = 6), Stau2 59kD (N = 5) and Stau2 52kD (N = 5) from RC normalized to level of starter and s6 for WT and FMR1-KO samples. H-K) The Quantification of enrichment of RG from RC between FMR1-KO and WT samples for s6 (N = 6), UPF1 (N = 6), Stau2 59kD (N = 5), and Stau2 52kD (N = 5).

### **Anisomycin and Puromycin Competition Indicates the similarity in WT and FMR1-KO RNA Granules**

Stalled ribosomes are paused at elongation and are structurally different than other translating ribosomes. High number of ribosomes found in RNA Granules are in the hybrid A/P and P/E configuration, a distinct state of the ribosome during elongation (Anadolu et al., 2023). Thus, by measuring the amount of altered state ribosomes in RNA Granules, we can know how effective stalling is in neurons. Puromycin and anisomycin are both translational inhibitors that bind to the A site of the ribosomes (Hansen et al., 2003; Garreau de Loubresse et al., 2014). Due to their overlapping binding site, anisomycin inhibits puromycin from binding to the ribosomes when both are present. However, it has been demonstrated that puromycylation of neuronal ribosomes isolated from cell culture and RNA Granules is resistant to anisomycin inhibition (Anadolu et al., 2024). This indicates the binding site for these translational inhibitors is altered

in the neuronal stalled ribosome. Thus, by looking at the percentage of puromycylation in the presence of anisomycin, we can estimate the number of ribosomes in this state.

We performed anisomycin and puromycin competition on ribosomes extracted through sucrose gradient to measure the amount of altered state ribosomes (Fig 2A). We first validated that puromycylation in non-neuronal ribosomes was not resistant to anisomycin through performing anisomycin and puromycin competition on rat liver ribosomes. Indeed, we saw a total inhibition of puromycin by anisomycin much like the effect previously seen on HEK cell culture (Fig 2B) (Anadolu et al., 2023). This conveyed that high centrifugation did not lead to puromycin's resistance to anisomycin and confirmed the neuronal specificity of this altered ribosomal state. We next examined if WT and FMR1-KO RG exhibit the same level of puromycylation resistance to anisomycin. We found that the two groups were comparable to each other (Fig 2C) with the quantification of the puromycylation revealed that WT and FMR1-KO RG both exhibited ~46% resistance to puromycin inhibition (Fig 2D). This proved that despite the absence of FMRP, the number of altered state ribosomes in these granules were unchanged.

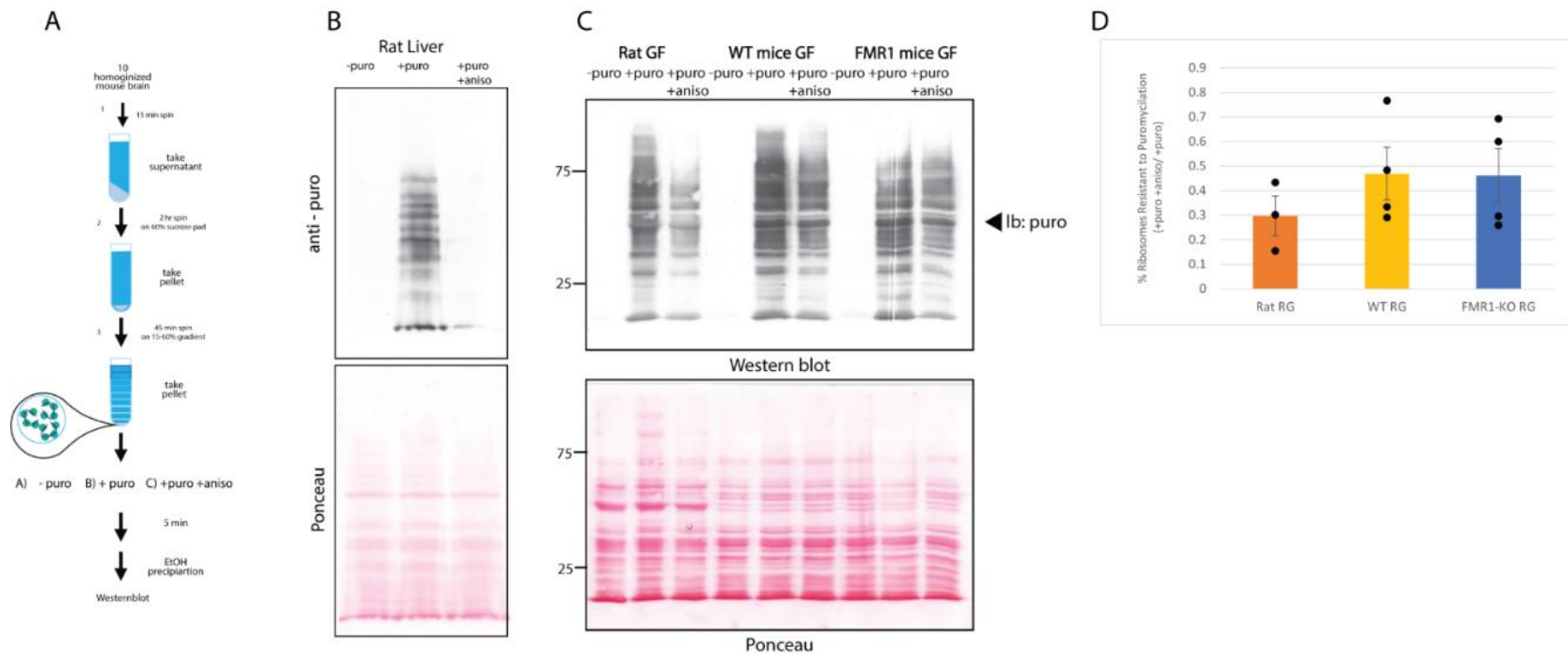


Figure 2. Anisomycin and Puromycin Competition in WT and FMR1-KO RG

A) A summary of protocol for anisomycin and puromycin competition on RNA Granules extracted from sucrose gradient fractionation. B) Top: Representative immunoblot that stained with anti-puro to showcase the inhibition of puromylation (100  $\mu$ M) by anisomycin (100  $\mu$ M) in liver polyribosomes. Bottom: Corresponding membrane stained with Ponceau before immunoblotting. The experiment was replicated twice with similar results. C) Top: Representative immunoblot that stained with anti-puro to showcase the inhibition of puromylation (100  $\mu$ M) by anisomycin (100  $\mu$ M) in Rat RG, WT mouse RG and FMR1-KO mouse RG. Bottom: Corresponding membrane stained with Ponceau before immunoblotting. D) Quantification of percentage puromylation resistant to anisomycin inhibition in Rat RG (N = 3), WT mouse RG (N = 4), FMR1-KO RG (N = 4). No significant difference was detected between groups (t-test p-value > 0.05).

## **Effects of Digestion and Mg<sup>2+</sup> on the Structure and Ribosomes Protected Fragments in RNA Granules**

To explore if the stalling sites of the ribosomes are altered by the loss of FMRP, we decided to inspect the Ribosomes Protected Fragments (RPF) of the stalled ribosomes. The protocol to extract RPF from WT and FMR1-KO RG was adopted from Anadolu et al., 2023 and followed by ribosomal footprinting protocol from Ingolia et al., 2014 (Fig 3A). However, the RPFs generated from the rat RG are generally above 35nt (Anadolu et al., 2023), while in other studies the RPF has a canonical size between 28nt and 32nt (Ingolia, 2014). In our previous study, the longer RPFs contained an extension past the RNA entrance site (3' end of RPF). It was not clear whether this was due to an extended conformation of the ribosome or an increased nuclease resistance in this region. It had previously been shown that hybrid-state ribosomes did not have an extended protection region (Wu et al., 2019) and our Cryo-EM structures did not show a large change in this region that could explain a larger ribosome protected fragment. Thus, we investigated whether this extended region could be cleaved off with more effective nuclease treatment.

Digestion from previous protocol was done at 4°C as several studies have found improved profiling with lower temperatures (Douka et al., 2021). We had optimized nuclease conditions for cleavage of ribosome clusters into monosomes (Anadolu et al 2023), but this might not have been optimal for removing the extending nucleotides. To determine if the extending nucleotides could be removed by increasing the effectiveness of nucleases, we performed digestion at room temperature instead of 4°C, and in addition, the 1µl RNase digestion was adjusted to the concentration of the RC or RG (see Methods).

The results showed that the excess region was sensitive to higher concentrations of nuclease. We replicated our previous result that the RPFs generated using our previous protocol were constantly above 35 nt (Anadolu et al., 2023). However, the RPFs generated from high nuclease treatment decreased the RPFs to around 28nt (Fig 3B). Interestingly, even with the high nuclease treatment, there was still a portion of RPFs that were around 35 nt (Fig 3B), Additionally, the majority of these mRNAs are noncoding mRNAs. The high nuclease treatment also displayed better quality than normal nuclease RPFs as seen by the higher percentage of RPFs in the coding region (CDS) (Fig 3C). Further examination of the region that was digested confirmed that the decrease in size was due to the loss of the 3' extension (Fig 3D). Another characteristic used to assess the quality of the RPFs is through their triplet periodicity, the attribute of how coding region displays three-nucleotide code in its mRNA. The triplet periodicity of the RPFs improved from ~40% in the normal nuclease treatment group to above 60% in high nuclease treatment group (3E). These results were consistent across RC, RG, WT and FMR1-KO groups.

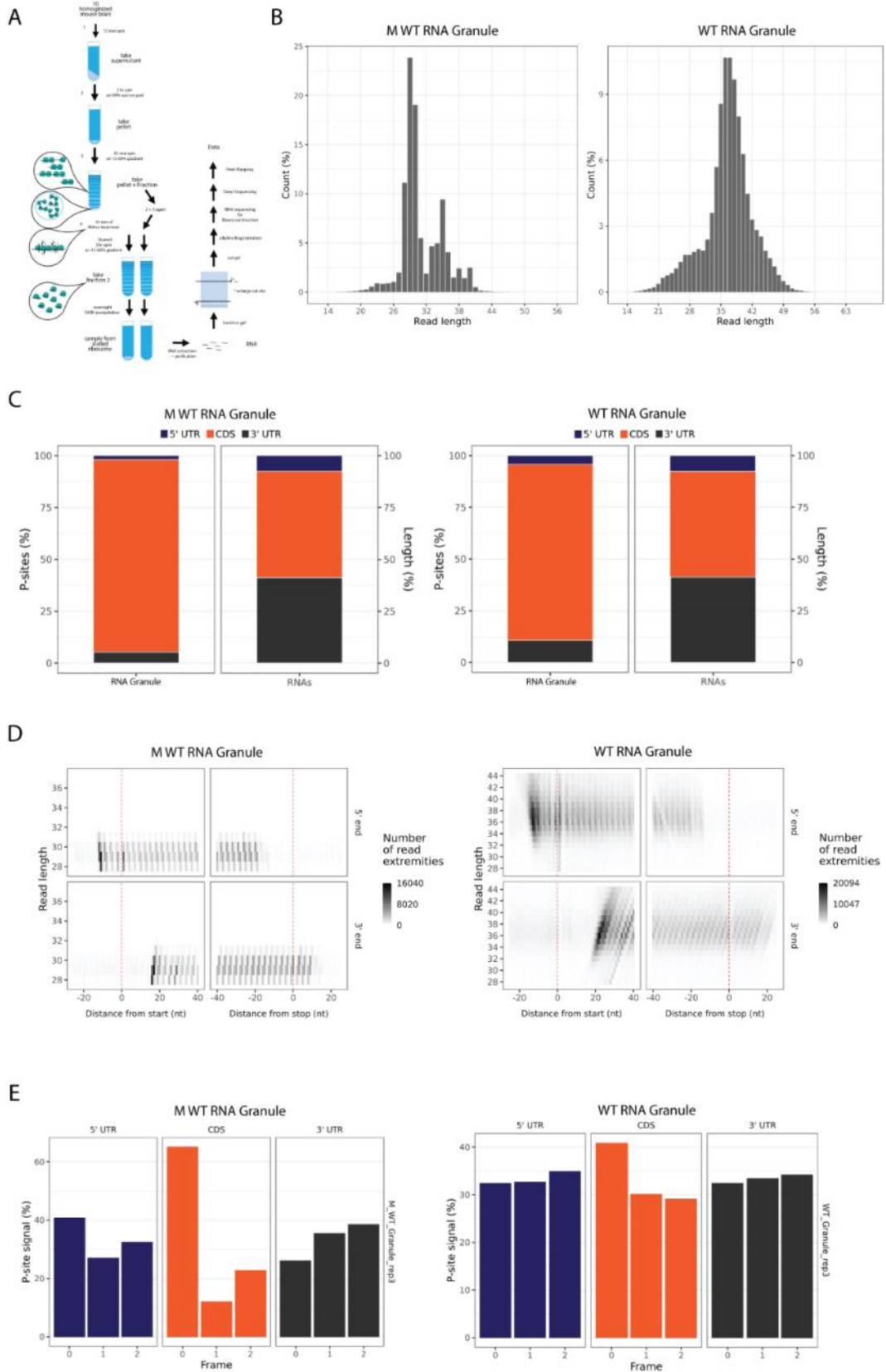


### Figure 3. High Nuclease Treatment Results on Ribosome Protected Fragments

A) A summary of protocol for ribosomal footprinting procedure. B) Representative image for size distribution of normalized footprint reads from high magnesium and high nuclease treatment group (M WT RNA Granule) and normal magnesium and normal nuclease treatment group (WT RNA Granule). C) Representative image for read coverage for M WT RNA Granule and WT RNA Granule. D) Representative image for the number of read extremities (shading) for each read length (Y-axis) based on the distance from start(left) to stop(right) with the 5' end (top) and 3' end (bottom) for M WT RNA Granule and WT RNA Granule. E) Representative image for the periodicity statistics for each read coverage RPFs. Though the representative images above only included one replicate for the result, the data are shown in all replicates for both WT and FMR1-KO groups.

An additional change from the previous protocol was in the concentration of  $MgCl_2$ . The previous solution used to extract the ribosomes (20mM Tris-HCl, pH7.4; 150mM NaCl; 2.5 mM  $MgCl_2$ ) has cellular level of  $Mg^{2+}$ . However, experiments that isolate the ribosomes in Cryo-EM typically use higher concentration magnesium due to low concentration of magnesium causing dissociation of small and large ribosomal subunits in bacteria (Yu et al., 2023). For polysome profiling, a study has shown high level of  $Mg^{2+}$  (30mM) causes less dissociation in yeast ribosomes (Bhattacharya et al., 2010). However, it has been reported that high concentration of magnesium in human ribosomes inhibited translation (Shenvi et al., 2005). If  $Mg^{2+}$  causes destabilization in normal translating ribosomes, it may have led to the lack of differences in Cryo-EM for rat RC and RG (Anadolu et al., 2023). Hybrid state ribosomes may have remained due to the A/P and P/E rotation of the tRNA serving as a stabilizer. In addition, previous study also had discrepancies with other published results (Anadolu et al., 2023). For example, the study that extracted neuronal ribosomes with 10mM  $Mg^{2+}$  observed the presence of eEF2 (Kraushar et al., 2021). Yet, eEF2 was absent in the RC from previous study (Anadolu et al., 2023). Thus, in addition to the high nuclease treatment, we also switched our solution to high  $Mg^{2+}$  solution

(20mM Tris-HCl, pH 7.4; 150 mM NaCl; 10 mM MgCl<sup>2+</sup>) for the second group of RPFs sample. Besides generating RPFs with high Mg<sup>2+</sup> solution, we also investigated these anomalies via generated RCs with cellular level Mg<sup>2+</sup> solution and high Mg<sup>2+</sup> solution for Cryo-EM analysis. The result showed that high Mg<sup>2+</sup> did not cause differences in the amount of hybrid state ribosomes observed (Fig. 4A). However, there was a slight decrease in the amount of 60S ribosomes. This indicated that the level of magnesium has little to no effect on our isolation of stalled neuronal ribosomes.

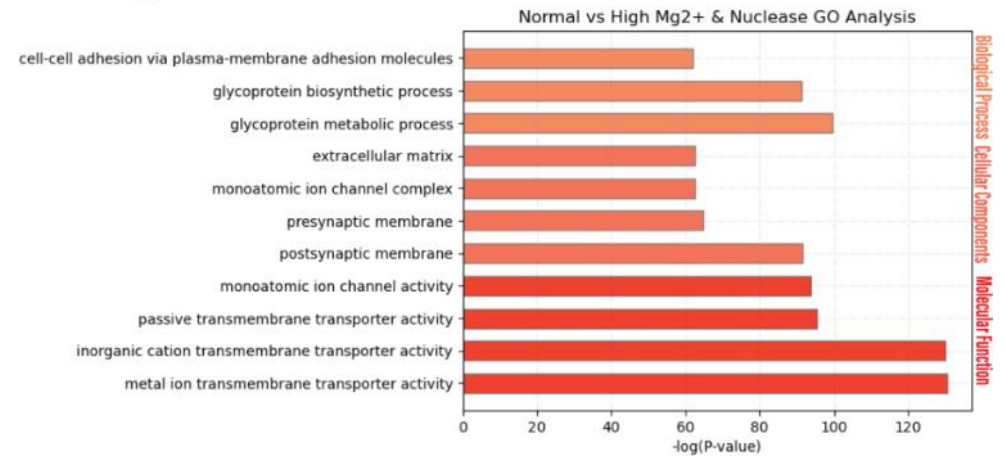
Due to the improved quality of RPFs and slight decrease in fragmented 60S ribosomes, we were inclined to focus on the high Mg<sup>2+</sup> and high nuclease group for bioinformatics analysis. However, we needed to determine if high Mg<sup>2+</sup> solution would alter our RPFs significantly and rendered it incomparable to the previous rat RG RPF results (Anadolu et al., 2023). Thus, we performed DEG analysis between high Mg<sup>2+</sup> and normal solution group to inspect the differences that high Mg<sup>2+</sup> cause. We performed GO Analysis on the significant genes, and it revealed that the high Mg<sup>2+</sup> RPFs lost a significant amount of mRNAs processes through the secretory pathway (Fig 4B). While previously we found that mRNAs for secretory proteins are low abundance in the RG compared to their abundance in whole brain RNA seq, they are enriched in the RG compared to RC (Anadolu et al., 2023), and this was proposed to be a contamination in the RG due to sedimentation of mRNAs that were being co-translationally inserted into the endoplasmic reticulum (ER). It appears that higher Mg<sup>2+</sup> concentrations reduced these mRNAs contamination and further solidified our focus on high Mg<sup>2+</sup> group for the analysis.

A

Cryo-EM Analysis of the Ribosomes Enriched from Cellular Level & High Mg<sup>2+</sup>

	Class 1: 80S with A/P and P/E tRNA	Class 2: 80S with P/P tRNA	Class 3: With only 60S subunit
RNA Granules (low Mg <sup>2+</sup> )	75 %	12 %	13 %
Ribosomal Cluster (low Mg <sup>2+</sup> )	73 %	17 %	9.7 %
Ribosomal Cluster (high Mg <sup>2+</sup> )	78.6 %	16%	5.4 %

B

Figure 4: Cryo-EM and GO Analysis of the Impact of High Mg<sup>2+</sup> on RNA Granules

A) Table of the Cryo-EM Analysis on ribosomes enriched from RG and RC with high Mg<sup>2+</sup> and cellular level Mg<sup>2+</sup>. B) Gene Ontology (GO) terms of the significant genes from the differential expression gene (DEG) analysis of WT RG and WT M RG for 1) top: Biological Function (Coral) 2) middle: Cellular Components (Tomato) and 3) bottom: Molecular Function (red).

## **Characterization of the Ribosome Protected Fragments of mRNAs in the WT and FMR1-KO RNA Granules through DEG and GO Analysis**

To analyze the mRNAs in the WT and FMR1-KO RNA Granules, we mapped the RPFs to its corresponding mRNA and investigated the identity of the mRNA. We first looked at the most abundant mRNAs in RGs. To compare the samples across different biological preparations, we calculated for the reads per kilobase per million mapped reads (RPKM), which normalized the mRNA count against the total RPFs mapped count and gene length. Ribosomal occupancy was calculated by the gene count of RG normalized against the total RNA extracted, which in this case came from sequencing the whole P5 homogenized brains. Though ribosomal occupancy is often referred to as translational efficiency, here we refer to it as ribosomal occupancy since the number of ribosomes per mRNA are unlikely to be related to translational efficiency in stalled ribosomes. By normalizing the RG RPFs against total brain mRNA, we can discern if an increase in the RG RPFs is due to a general abundance of mRNA in P5 brains or if it is particular to our RNA Granules. Lastly, we calculated for enrichment between RG and RC to determine the groups of mRNAs that are selected into RG.

When comparing GO Analysis to identify which groups of mRNAs dominated the WT and FMR1-KO RG, we did not see considerable differences. The GO Analysis on the top 500 abundant genes in the WT and FMR1-KO RG showed cytoskeleton groups to be the most abundant (Fig 5). This matched with the previous result from rat RG (Anadolu et al., 2023). For occupancy in RG, GO Analysis revealed WT and FMR1-KO RG still were most occupied by cytoskeleton related mRNAs, such as microtubule, microfilament, and actin filament (Fig 5). In addition, both WT and FMR1-KO RG were highly occupied in mRNA processing, like splicing and localization, and ribosome genesis related mRNAs (Fig 5). This also replicated the previous

result (Anadolu et al., 2023). We also accessed the most enriched mRNAs in WT and FMR1-KO RG. We found that much like abundance, occupancy, the WT and FMR1-KO RG were both highly enriched in cytoskeleton. Curiously, FMR1-KO enrichment had more significant GO Analysis (MF: 89, BP: 398, CC: 127) compared to WT enrichment (MF: 27, BP: 57, CC: 32), which indicated that there was a wider difference between FMR1-KO RG and RC. However, overall WT and FMR1-KO RG mRNA seemed similar.

We next compared the specific effects of FMRP on RG through performing DEG Analysis on FMR1-KO and WT on RG abundance, occupancy, and enrichment. There were only 2 protein coding genes that were significantly difference between the abundance of FMR1-KO and WT in protein coding genes – FMR1 and Wdfy1. There were no significantly different genes between WT and FMR1-KO RG occupancy and enrichment.

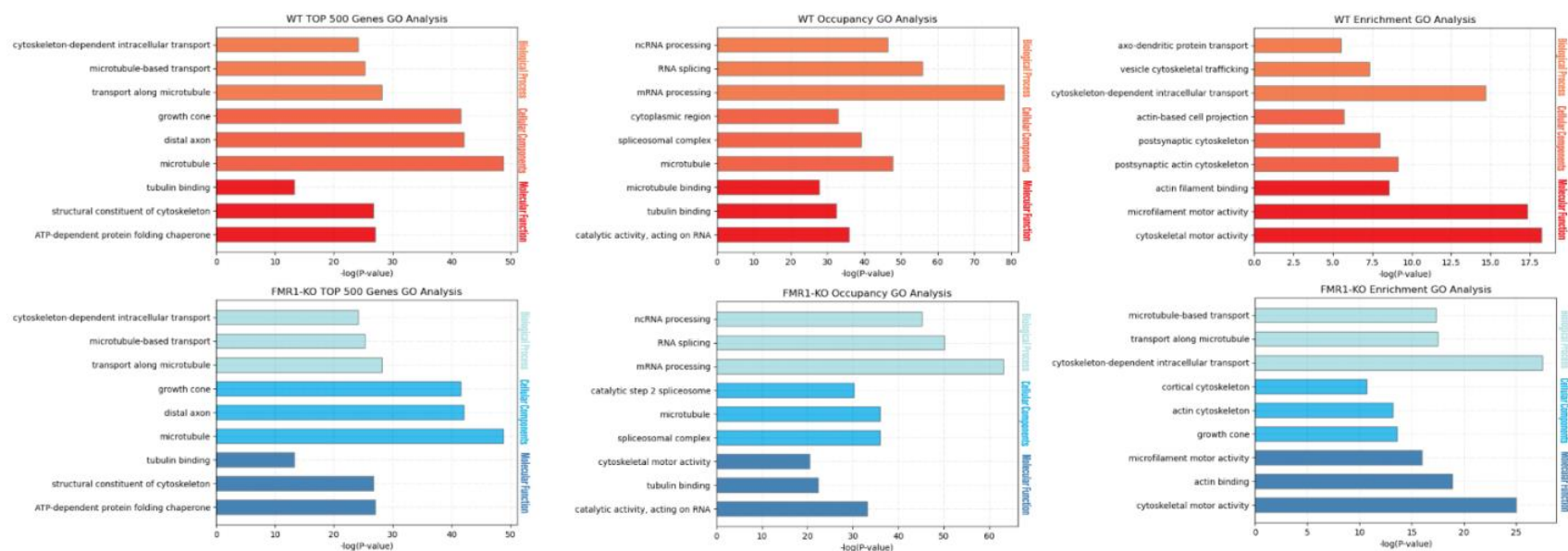


Figure 5: GO Analysis of WT and FMR1-KO Analysis in Abundance, Enrichment and Occupancy

TOP: GO terms of the WT M RG in 1) left: top 500 most abundance gene (CC) 2) middle: occupancy and 3) right: enrichment. Each graph has the ontology match for Biological Function (top and coral), Cellular Components (middle and Tomato), and Molecular Function (bottom and red). Bottom: GO terms of the FMR1-KO M RG in 1) left: top 500 most abundance gene (CC) 2) middle: occupancy and 3) right: enrichment. Each graph has the ontology match for Biological Function (top and turquoise), Cellular Components (middle and sky blue), and Molecular Function (bottom and steel blue).

## **Comparison of the Ribosome Protected Fragments of mRNA in the WT and FMR1-KO Analysis to Selected Datasets**

In our previous study using rat RGs, we found increased RPFs, ribosome occupancy and enrichment in the RG for subsets of mRNA linked to stalling (Shah et al, 2020) and for mRNAs that had been previously identified that FMRP associate to using HIT-CLIP (Darnell et al; Maurin et al). We first examined the number of mRNAs that are associated with ribosomes resistant to HHT runoff (Shah et al., 2020). The WT and FMR1-KO were significantly abundant, occupied and enriched in mRNA resistant to run-off (Fig 6). This mimicked the previous results from Rat RNA Granule (Anadolu et al., 2023). More importantly, it showed that the loss of FMRP did not affect the mRNAs related to the ribosomes that remained after run-off. Next, we investigated FMRP associated mRNAs through assessing FMRP-Clipped mRNA in WT and FMR1-KO R (Darnell et al., 2011; Maurin et al., 2018). FMRP-Clip were identified by cross-linking FMRP with mRNA, fragmenting the mRNA, immunoprecipitating the mRNA associated with FMRP, and sequencing it (Darnell et al., 2011; Maurin et al., 2018). The mRNA fragmentations are larger than FMRP itself, thus it does not provide the direct binding site of the FMRP, but it does provide potential sites where FMRP is associated to. We found that FMRP-Clipped mRNAs were highly abundant, enriched and occupied in WT RG (Fig 6A, Fig 6C, Fig 6E), which replicated the previous results obtained from the rat RG (Anadolu et al., 2023). Interestingly, while still significant, there appeared to be a decrease in the relative abundance of these mRNAs in the KO (Fig 6B) and particularly, these groups did not show an increase in occupancy compared to total mRNAs (Fig 6D). This suggested there were less ribosomes on the FMRP-Clipped mRNAs when FMRP was removed. However, despite the strong enrichment of FMRP in the RG compared to the RC, the FMRP clipped RNAs were still highly enriched in the

RG, to a level comparable to the WT (Fig 6F). We next examined the specific effect of FMRP on these subsets of mRNA via calculating the fold change differences in abundance, occupancy and enrichment of WT and FMR1-KO RG. The loss of FMRP significantly affected the abundance and occupancy of FMRP-Clipped mRNAs in WT and FMR1-KO RG (Fig 7A, 7B), but not their enrichment between RG and RCs (Fig 7C). This was because the abundance of these mRNAs in the RCs was also reduced (Fig 7D). Thus, even though the loss of FMRP did not affect the overall trend of increased mRNA relating to ribosomes resistant to run-off and FMRP-Clipped mRNAs, the elimination of FMRP reduced the amount of FMRP-Clip.

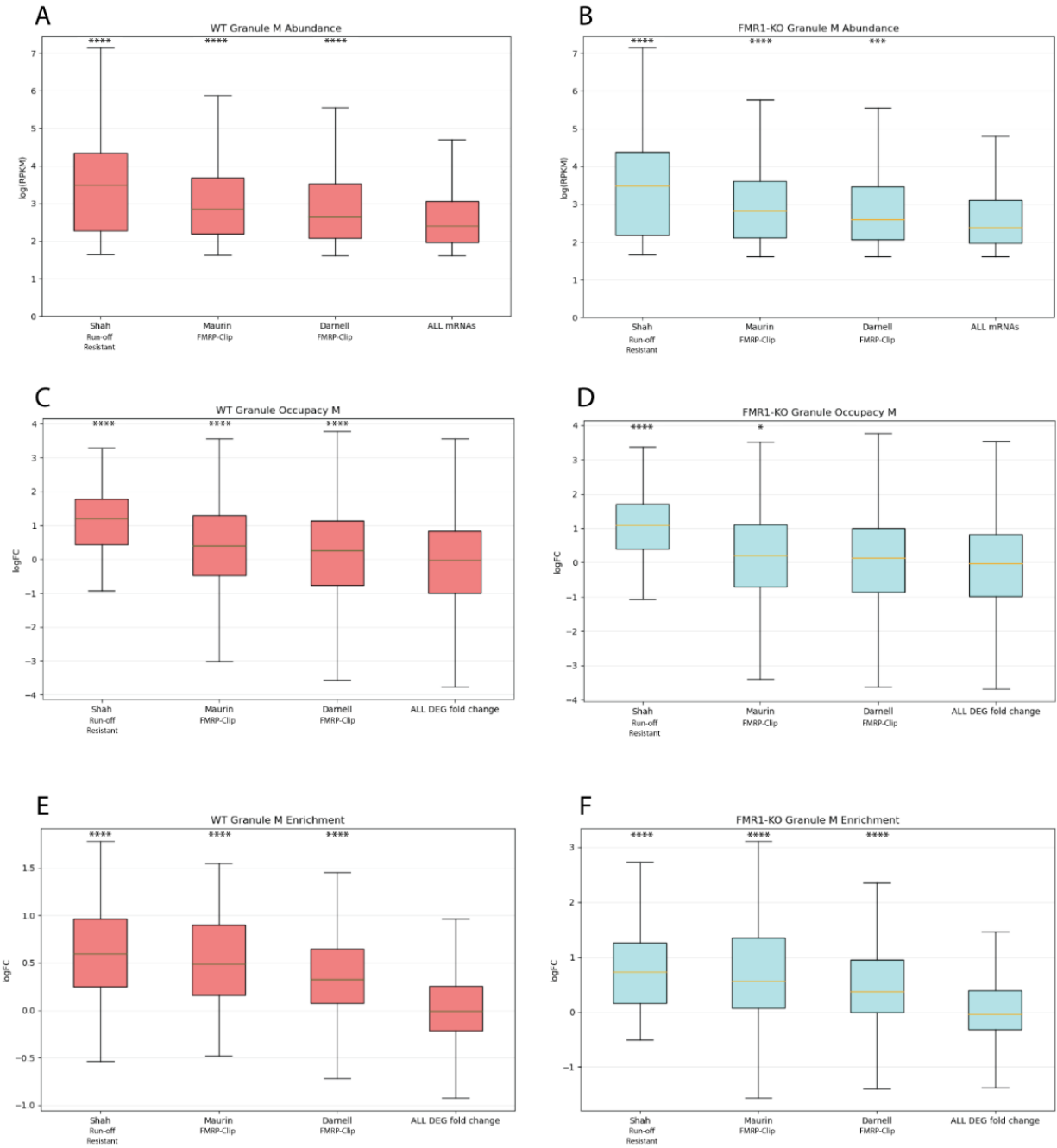


Figure 6: Correlation Analysis to RPFs from Ribosomes Resistant to Run-off and FMRP-Clipped

A) WT Granule abundance, B) FMR1-KO Granule M abundance, C) WT Granule Occupancy, D) FMR1-KO Granule Occupancy, E) WT Granule Enrichment, and F) FMR1-KO Granule Enrichment in comparison to mRNAs associated to ribosome resistant of initiation inhibitor run-off (Shah et al., 2020) and FMRP-CLIPPed mRNAs (Maurin et al., 2018; Darnel et al., 2011). P-

values from each trait were calculated by performing Student's t-test between the mRNAs that matched to the published dataset and the ones that did not.

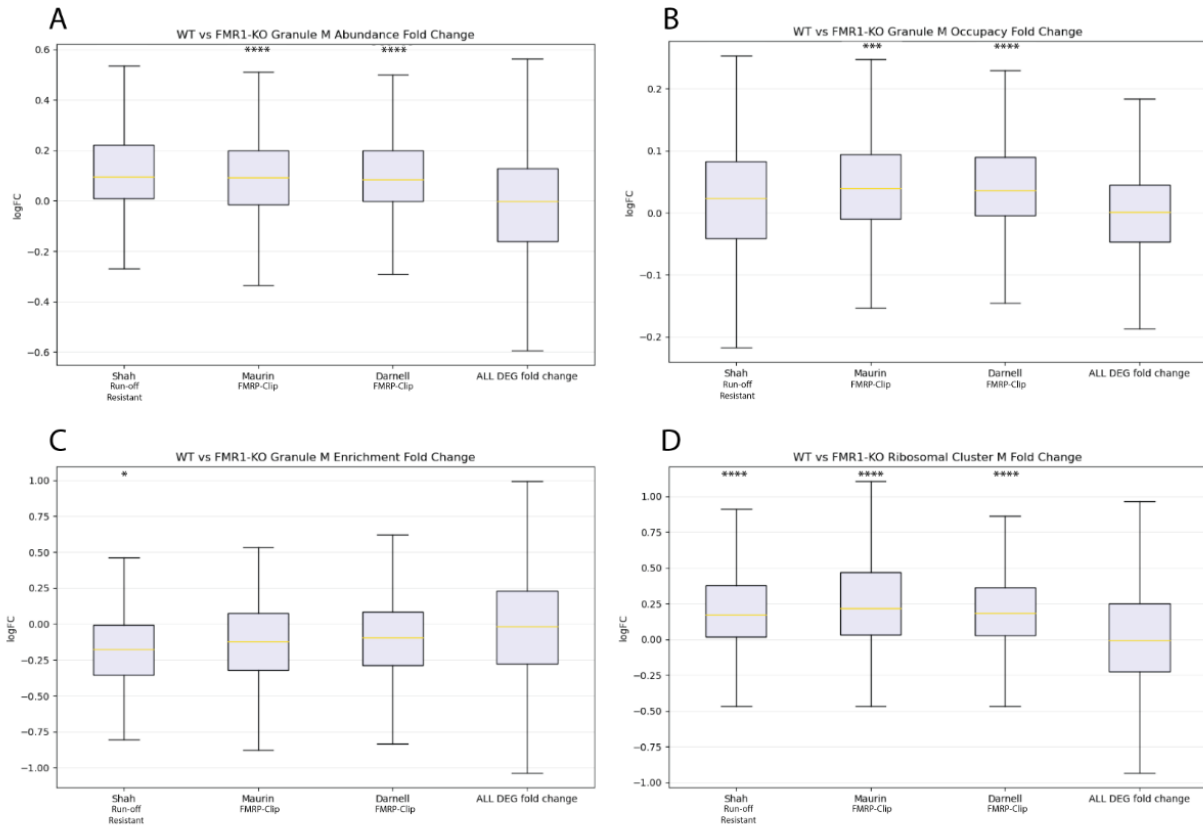


Figure 7: Correlation Analysis of the Fold Change between WT and FMR1-KO to RPFs from Ribosomes Resistant to Run-off and FMRP-Clipped

Fold change between A) WT and FMR1 fold change in RG abundance, B) WT and FMR1 fold change in RG occupancy, C) WT and FMR1 fold change in RG enrichment, and D) WT and FMR1 fold change in RC abundance in comparison to mRNAs associated to ribosome resistant of initiation inhibitor run-off (Shah et al., 2020), FMRP-CLIPPed mRNAs (Maurin et al., 2018; Darnel et al., 2011). P-values from each trait were calculated by performing Student's t-test between the mRNAs that matched to the published dataset and the ones that did not.

We also investigated how the loss of FMRP altered the mRNAs regulated by elongation or initiation in our RNA Granules. There was a significantly abundant and occupied number of mRNAs related to proteins regulated by eEF2K in the WT and FMR1-KO RG (Fig 8A, 8B, 8C, 8D) (Kenney et al., 2016). However, the statistical significance of eEF2K related mRNA was no longer present in FMR1-KO enrichment (Fig 8F), which implied that the eEF2K related mRNA was proportional between RC and RG when FMRP was eliminated. For the translation initiation pathway, we saw a weak to no significant correlation in the abundance, occupancy and enrichment of mRNA regulated by mGluR-LTD induced initiation (Fig 8) (Di Prisco et al., 2014). The WT RG for abundance, enrichment and occupancy in mRNA regulated by eIF4E phosphorylation diverged from the study on rat RG, where there was no decrease in the abundance of eIF4E phosphorylated mRNA, and a small but significant increase in eIF4E phosphorylated mRNA in occupancy and enrichment (Fig 8A, Fig 8C, Fig 8E) (Amorim et al., 2018, Anadolu et al., 2023). This trend was similar in WT and FMR1-KO RG (Fig 8B, Fig 8D, Fig 8F). For mTOR related mRNA, there was a significant decrease in WT and FMR1-KO RG in occupancy and enrichment (Fig 8C, Fig 8D, Fig 8E, Fig 8F) (Thoreen et al., 2012) similar to what was seen previously (Anadolu et al., 2023). When analyzing the differences FMRP caused by performing DEG analysis between the WT and FMR1-KO data, we observed a decrease in the abundance and occupancy of the mRNA regulated by eEF2K, which had a high overlap with FMRP- Clipped mRNAs (Fig 9A, Fig 9B). Interestingly, there was a small but significant discrepancy between mRNAs regulated by the mTOR pathway in enrichment (Fig 9C), but this change seemed to be mainly mediated by changes in the abundance of RCs (Fig 9D). Overall, the loss of FMRP did not alter the trend where RG is enriched in mRNA regulated by the elongation

pathway, and there were only small changes in the amount of RPFs in mRNAs regulated by initiation in the absence of FMRP.

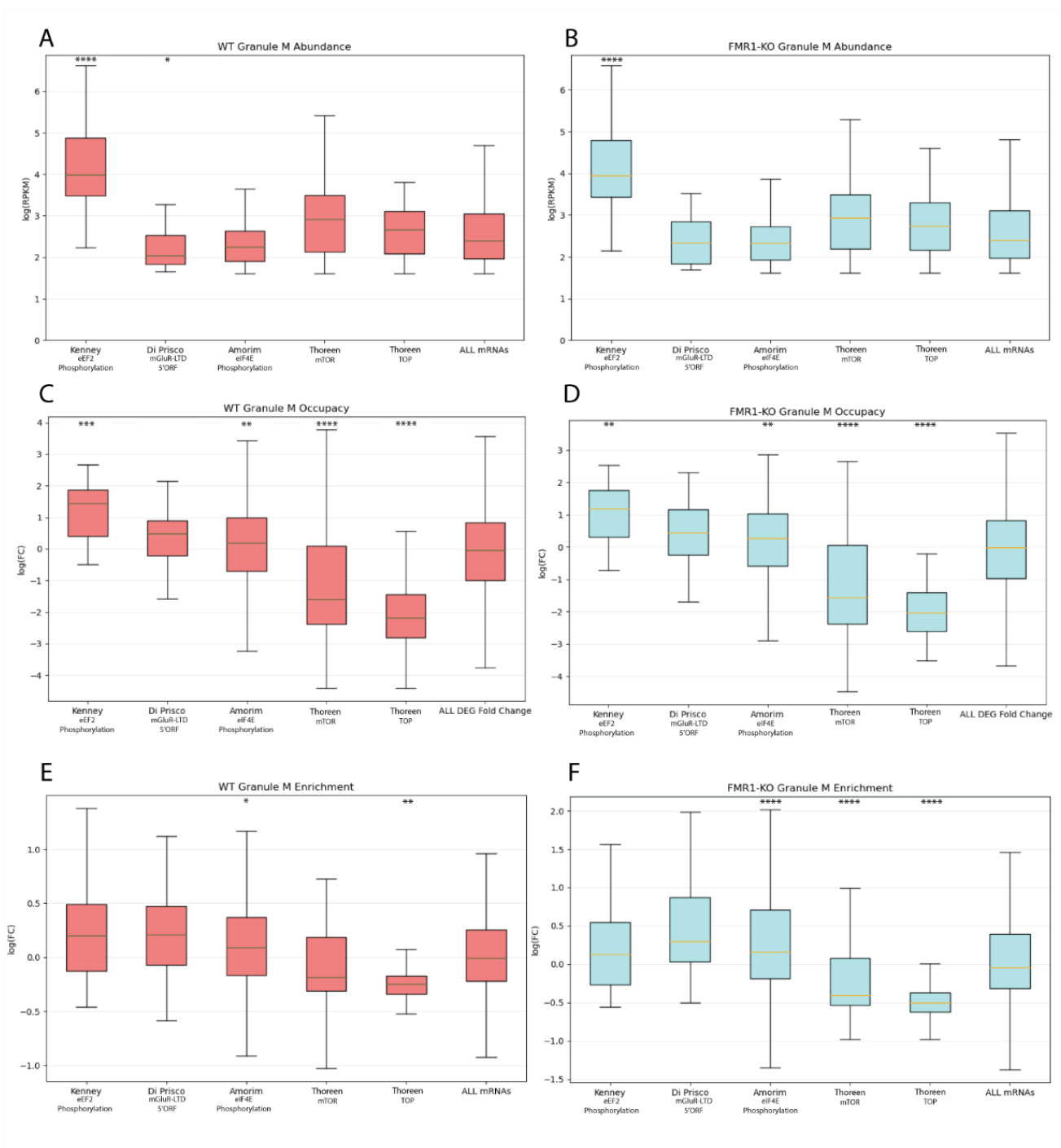


Figure 8: Correlation Analysis to mRNAs Regulated by Initiation and Elongation

A) WT Granule abundance, B) FMR1-KO Granule M abundance, C) WT Granule Occupancy, D) FMR1-KO Granule Occupancy, E) WT Granule Enrichment, and F) FMR1-KO Granule Enrichment in comparison to mRNAs regulated by eEF2K (Kenney et al., 2016), 5'ORFs of mRNAs produced mGluR-LTD stimulation, (Di Prisco et al., 2014), eIF4E phosphorylation

(Amorim et al., 2018), and mRNA regulated by the mTOR pathway (Thoreen et al, 2012). P-values from each trait were calculated by performing Student's t-test between the mRNAs that matched to the published dataset and the ones that did not.

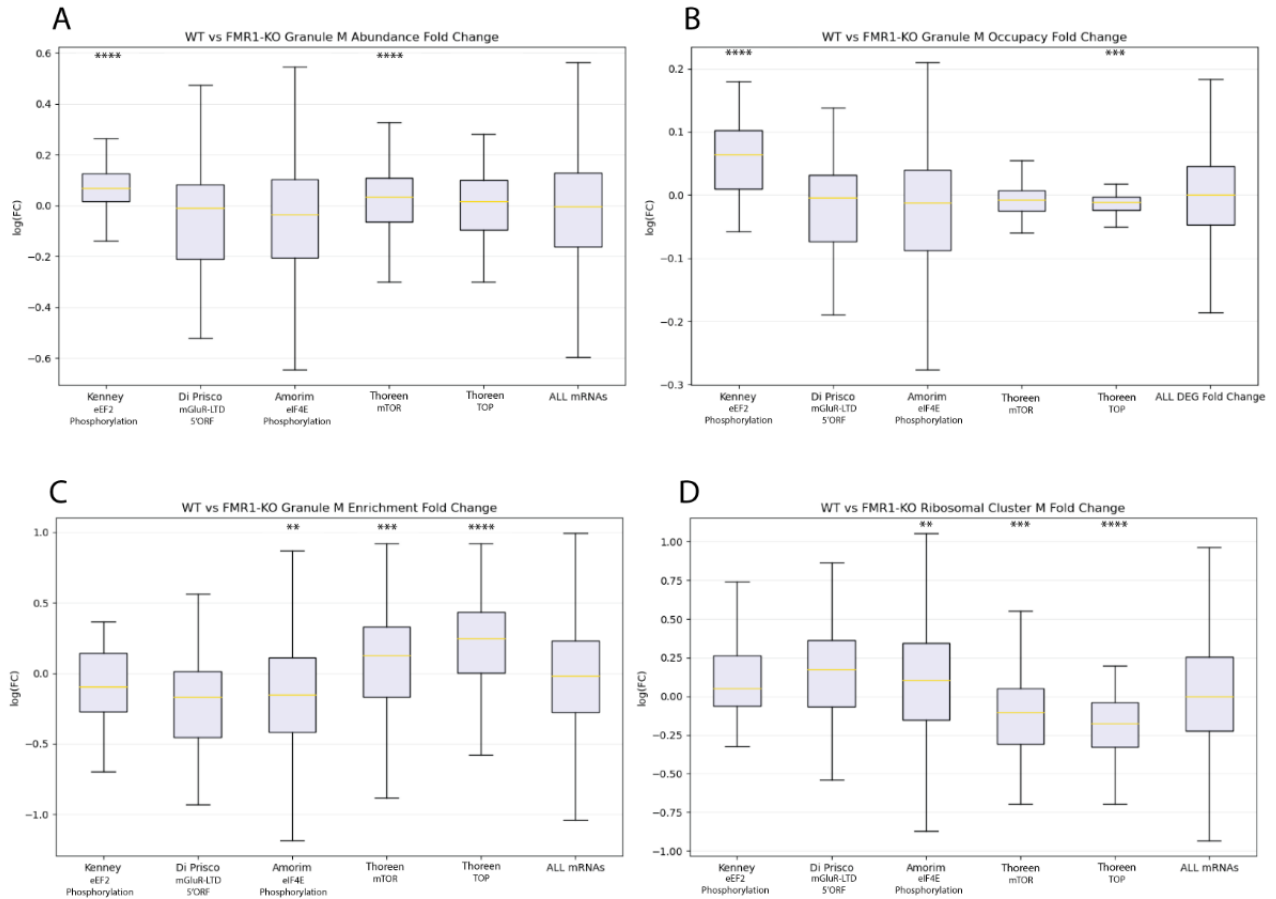


Figure 9: Correlation Analysis of the Fold Change between WT and FMR1-KO to mRNAs Regulated by Initiation and Elongation

Fold change between A) WT and FMR1 fold change in RG abundance, B) WT and FMR1 fold change in RG occupancy, C) WT and FMR1 fold change in RG enrichment, and D) WT and FMR1 fold change in RC abundance in comparison to mRNAs regulated by eEF2K (Kenney et al., 2016), 5'ORFs of mRNAs produced mGluR-LTD stimulation, (Di Prisco et al., 2014), eIF4E phosphorylation (Amorim et al., 2018), mRNA regulated by the mTOR pathway (Thoreen et al, 2012) P-values from each trait were calculated by performing Student's t-test between the mRNAs that matched to the published dataset and the ones that did not.

A study had identified the mRNAs particularly translated by monosomes or polysomes in neurons (Biever et al., 2020). We were interested in how FMR1-KO affected the FMR1-KO affected the amount of RPFs on these subsets of mRNA. The result showed that the subset of mRNAs preferentially translated by monosomes were abundant, highly occupied and enriched in both the WT and FMR1-KO RG (Fig 10). On the other hand, there was no longer a significance in the abundance for mRNAs preferentially translated by polysomes, unlike the previous result (Fig 10A, 10B) (Anadolu et al., 2023). In fact, we observed a drastic reduction in the enrichment of mRNAs translated by polysomes in both the WT and FMR1-KO RG (Fig 10E, 10F). There was only a small significance in the enrichment for secretory mRNAs, unlike the previous study (Anadolu et al., 2023) (Fig 10A, 10B, 10C, 10D), which was consistent with the effect of magnesium in the GO Analysis result (Fig 4B). When analyzing the fold change between the WT and FMR1-KO samples, the most notable difference was the drastic decrease in mRNA translated by monosomes when FMRP was lost (Fig 11). However, this decrease can be mainly attributed to the genes that overlapped with FMRP-Clipped mRNAs.

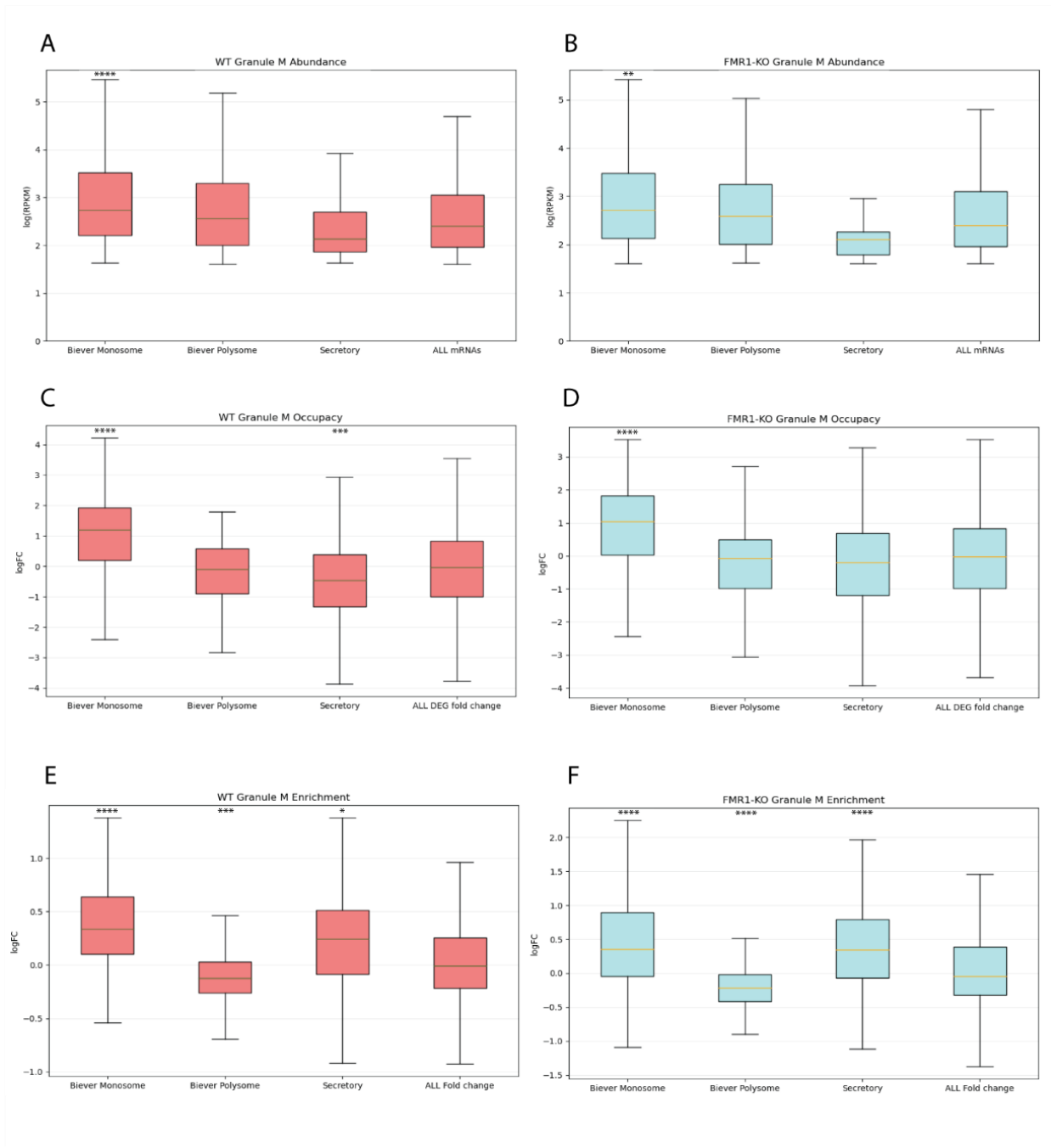


Figure 10: Correlation Analysis to mRNAs Translated by Monosome, Polysome and Secretary Proteins

A) WT Granule abundance, B) FMR1-KO Granule M abundance, C) WT Granule Occupancy, D) FMR1-KO Granule Occupancy, E) WT Granule Enrichment, and F) FMR1-KO Granule Enrichment in comparison to mRNA translated by monosomes and polysomes in the neuropil (Biever et al., 2020), and secretary mRNAs. P-values from each trait were calculated by

performing Student's t-test between the mRNAs that matched to the published dataset and the ones that did not.

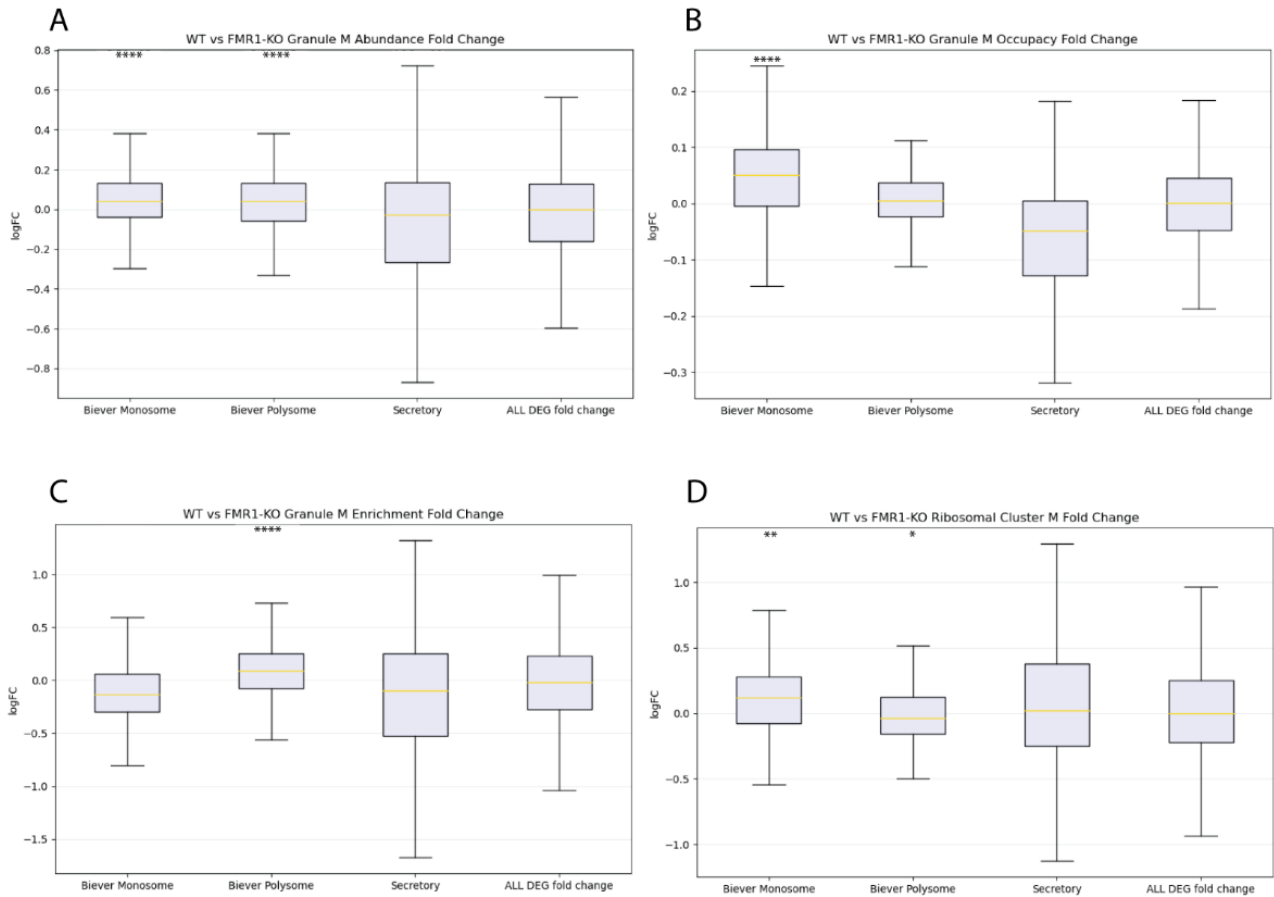


Figure 11: Correlation Analysis of the Fold Change between WT and FMR1-KO to mRNAs Translated by Monosome, Polysome and Secretory Proteins

Fold change between A) WT and FMR1 fold change in RG abundance, B) WT and FMR1 fold change in RG occupancy, C) WT and FMR1 fold change in RG enrichment, and D) WT and FMR1 fold change in RC abundance in comparison to mRNA translated by monosomes and polysomes in the neuropil (Biever et al., 2020) and secretory mRNAs. P-values from each trait were calculated by performing Student's t-test between the mRNAs that matched to the published dataset and the ones that did not.

Fragile X syndrome is the largest known genetic cause for autism spectrum disorder. Thus, we investigated how the loss of FMRP affected the mRNAs related to autism spectrum disorder identified by the SFARI database. There was a significant abundance of autism related mRNAs no matter if it was related to FMRP or not in both the WT and FMR1-KO RG, which was similar to the previous result (Fig 12A, 12B) (Anadolu et al., 2023). However, the WT and FMR1-KO RG were more occupied in non-FMRP than FMRP correlated autism related mRNA (Fig 12C, 12D). When looking into the specific differences between the two, the non-FMRP related autism mRNAs were not affected. On the other hand, the FMRP related autism genes were significantly altered by the loss of FMRP in abundance, occupancy, and enrichment (Fig 13A, 13B, 13C). The results from autism related genes again demonstrated that FMRP does not cause differences in non-FMRP associated autism mRNAs but does cause a decrease in FMRP related autism mRNAs.

Previously, it had been revealed that UPF1 is a key player in stalled ribosomes formation (Graber et al., 2013; Graber et al., 2017) which is also a major player for NMD pathway (Park et al., 2020). In addition, it has been reported recently that loss of FMRP caused hyperactivation in NMD pathway (Kurosaki et al., 2021). Thus, we decided to examine the correlation between the NMD regulated mRNAs in RNA Granules to 1) confirm if RG was contaminated by NMD pathway, and to 2) examine if FMRP caused the differences in NMD related mRNAs. There seemed to be a significant decrease in the abundance and occupancy of NMD related mRNAs for both the WT and FMR1-KO RG (Fig 12A, 12B, 12C, 12D). This solidified that our RNA Granules did not contain NMD regulated mRNAs. More importantly, it showcased how the loss of FMRP did not increase NMD related mRNAs in RNA Granules. We also examined the mRNAs encoding mitochondrial proteins mRNA in our granules. There was no significance

between the mRNAs overlapped in mitochondrial protein mRNAs in abundance and occupancy of RG. Surprisingly, we detected a significant decrease in the enrichment of these mRNAs in the FMR1-KO RG (Fig 12). This was confirmed when directly analyzing the differences FMRP caused, we observe that mitochondrial mRNAs were significantly altered in RG abundance, RC abundance, and RG enrichment (Fig 13). In particular, these mRNAs decreased in abundance in the RGs, but increased their abundance in RCs when FMRP was knocked down. This showed that when FMRP is lost, the mitochondrially translated mRNAs shift in their distribution between the RGs and RCs.

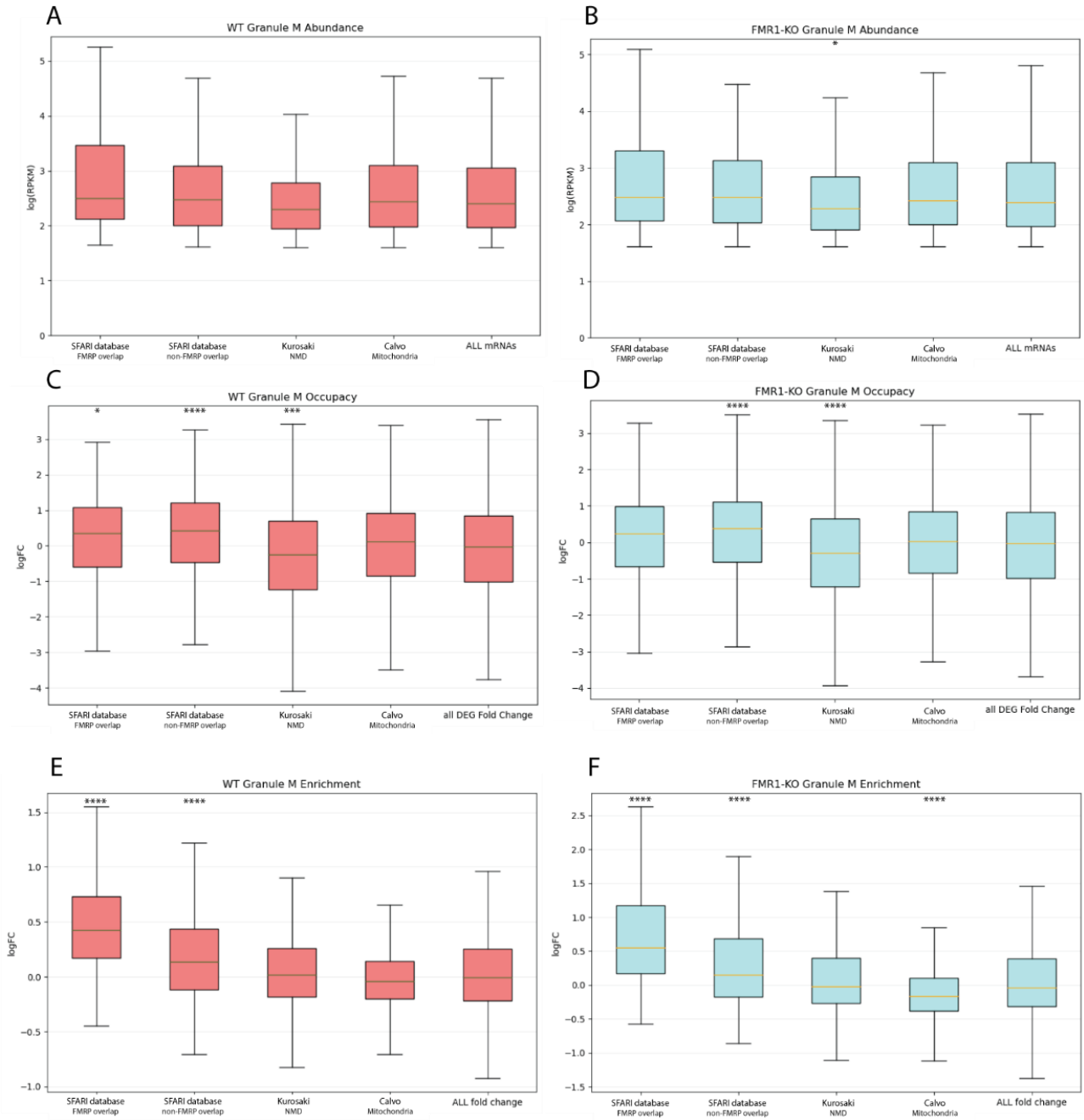


Figure 12: Correlation Analysis to Other Datasets of Interest

A) WT Granule abundance, B) FMR1-KO Granule M abundance, C) WT Granule Occupancy, D) FMR1-KO Granule Occupancy, E) WT Granule Enrichment, and F) FMR1-KO Granule Enrichment in comparison to autism related genes from the SFARI database, mRNA regulated by the NMD pathway (Kurosaki et al., 2021) and mitochondrial mRNA from the mitocarta 2.0 database. The SFARI group was divided into the ones associated with FMRP-CLIP and the ones

not associated. P-values from each trait were calculated by performing Student's t-test between the mRNAs that matched to the published dataset and the ones that did not.

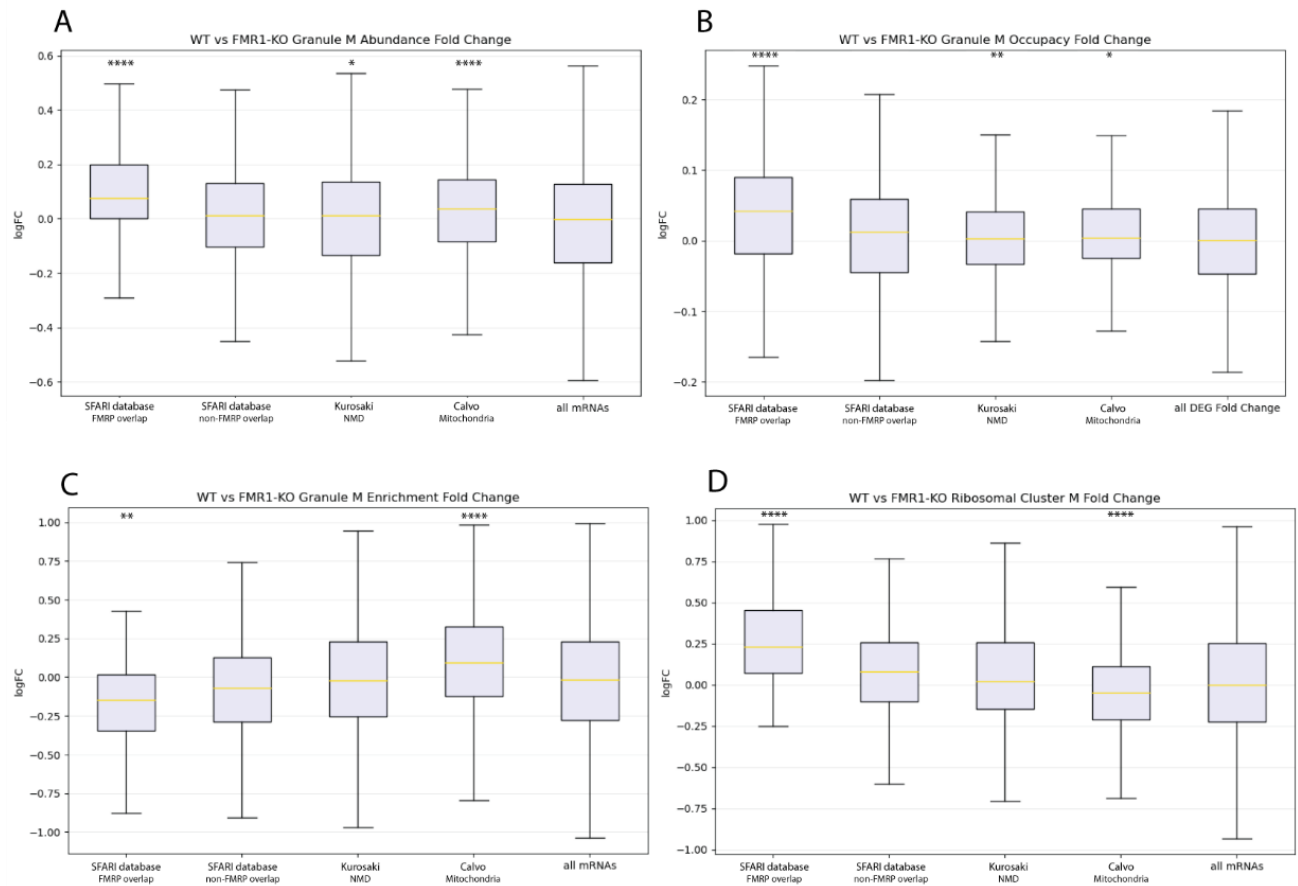


Figure 13. Correlation Analysis of the Fold Change between WT and FMR1-KO to Other Datasets of Interest

Fold change between A) WT and FMR1 fold change in RG abundance, B) WT and FMR1 fold change in RG occupancy, C) WT and FMR1 fold change in RG enrichment, and D) WT and FMR1 fold change in RC abundance in comparison to autism related genes from the SFARI database, mRNA regulated by the NMD pathway (Kurosaki et al., 2021) and the mitochondrial mRNA from the mitocarta database. The SFARI group was divided into the ones associated with FMRP-CLIP and the ones not associated. P-values from each trait were calculated by performing Student's t-test between the mRNAs that matched to the published dataset and the ones that did not.

## Peak Analysis on the WT and FMR1-KO RNA Granules

The previous result showcased that the stalled ribosomes preferentially bound to FMRP related mRNA motifs (Anadolu et al., 2023), such as the WGGA motif (Ascano et al., 2012; Anderson et al., 2016). Thus, to inquire if the loss of FMRP altered the location of stalled ribosomes, the abundance of individual stalling sites was calculated. We referred to these sites as the peaks. However, there were certain issues with the reproducibility of previous peak selections (Anadolu et al., 2023). The peaks previously were selected through marking the inflection point within the abundances of RPFs. If these regions overlap between 85%- 90% across the majority of the replicates, it was selected. In addition, the height of the amplitude for the peaks must be higher than the average RPKM. Though the criteria for peak selection were stringent, it was hard to reproduce these peaks in additional experiments. Thus, the peaks for our analysis were selected through identifying the highest point after each read was compiled on top of each other for each transcript. The zenith of an abundance site for the reads must be 4x higher than the average of the total transcript to be marked as peaks. In addition, the peak must be present in all the replicates, which meant the peaks' sequences must be within 6 nts for all replicates (Fig 14A).

Through this method, we found 1392 peaks present in all six samples. In contrast there were only 317 peaks present in the WT samples, and 225 peaks in the FMR1-KO samples. This implied a high overlap in the number of peaks between the WT and FMR1-KO RPFs. Interestingly, when we performed HOMER Analysis on WT RG RPFs and FMR1-KO RG RPFs, the WGGA motifs were no longer observable (Fig 14C). Yet, when performing HOMER Analysis of the combined peaks from WT and FMR1-KO RPFs, the WGGA peaks were

identified (Fig 14C). These results suggested that the stalling sites were unchanged by the loss of FMRP.

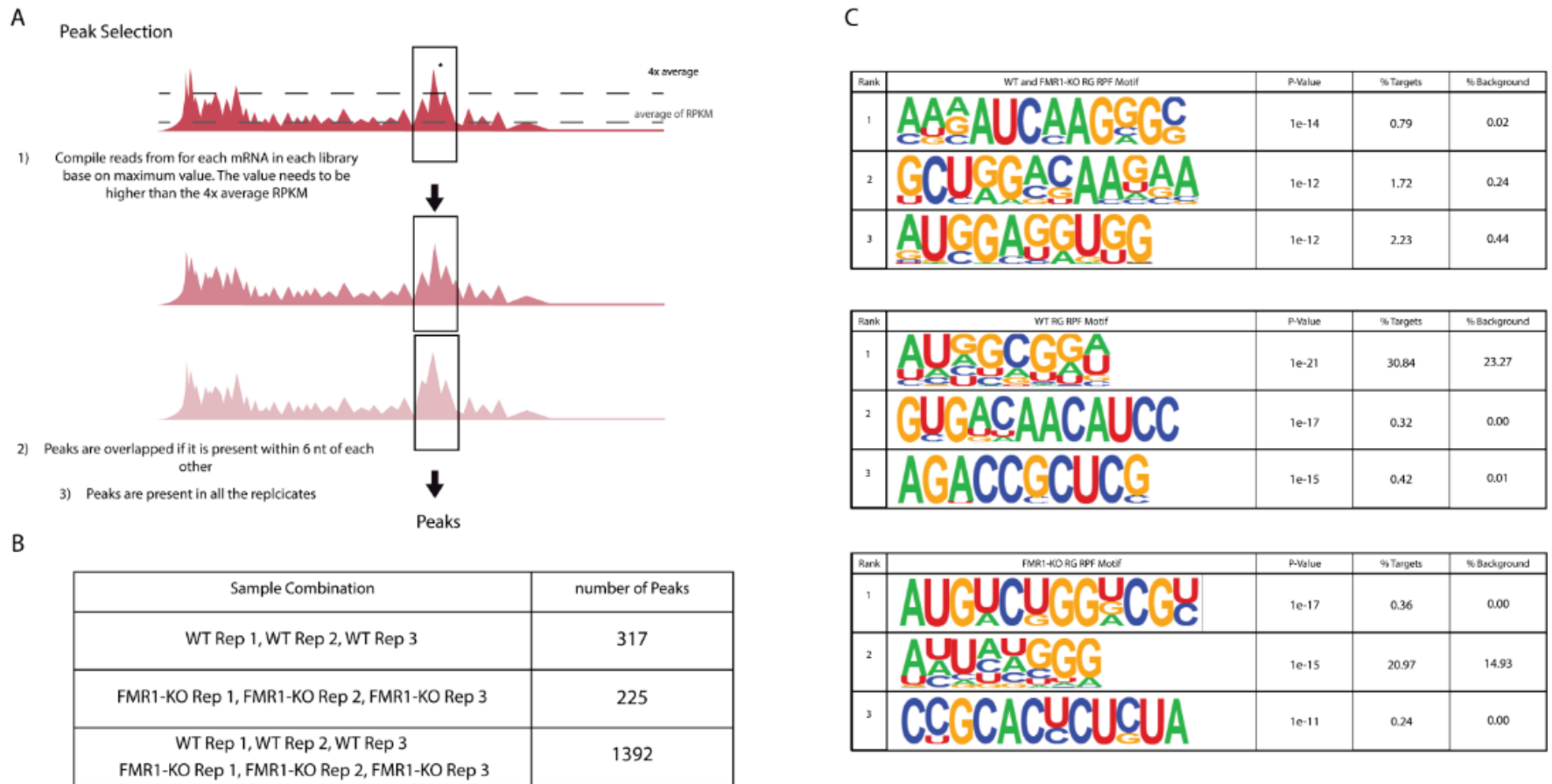


Figure 14: Peaks Analysis of WT and FMR1-KO RG

A) A summary for peak selection process from ribosome protected fragments (RPF). B) Results of the number of peaks between replicates of WT RNA Granule (N = 3), FMR1-KO RNA Granule (N = 3) and combined (N = 6). C) HOMER Analysis showed the top 3 consensus motif generated from WT RG, FMR1-KO RG and combined peaks.

## **Conclusion & Discussion**

No gross changes in the characteristics of RNA granules were detected in the absence of FMRP. The enrichment of UPF1 was comparable between the two groups (Fig 1). The amount of altered state ribosomes examined by anisomycin and puromycin competitions were equivalent between the WT and FMR1-KO RG (Fig 2). The mRNA packaged into the RNA Granules with or without FMRP showed little to no statistically significant differences, and there were no differentially expressed genes when comparing mRNAs in RNA granules between WT and FMR1-KO mice (Fig 5, 6, 8, 10, 12). We observed an enrichment in FMRP related mRNA dataset, mRNA related to ribosomes resistant to runoff, eEF2k regulated proteins and a de-enrichment of initiation pathway regulated mRNAs in both the WT and FMR1-KO RG (Fig 5, 6, 8, 10, 12), which replicated the result from rat RNA granules (Anadolu et al., 2023). Finally, most peaks observed in the coverage of RPFs were found to overlap in both WT and FMR1-KO mice (Fig. 14). However, there were subtle changes in the mRNAs present in the RNA granules in the absence of FMRP. When we concentrated on the mRNAs identified in FMRP Clips, the abundance and occupancy of these mRNAs in RNA granules and ribosome clusters decreased when FMRP is lost (Fig 7). It seems that when FMRP is lost there is less overall stalling on the mRNAs clipped by FMRPs, without affecting the stalling sites and the enrichment of FMRP-Clipped mRNA in the RNA Granules. Thus, we conclude that FMRP is not essential for stalled ribosomes formation.

While overall, the loss of FMRP had minor effects on the overall distribution of RPFs seen by the lack of DEGs in these experiments, when looking at subsets of mRNAs, we can detect more subtle effects of FMRP on subsets of mRNAs. In particular, mRNAs associated with FMRP based on previous CLIP studies have less RPFs in both clusters and granules, suggesting

that the stalling of these mRNAs is decreased (Fig. 7). Other datasets that were altered significantly by the absence of FMRP, such as the proteins regulated by eEF2K (Kenney et al., 2016) and monosome mRNA (Fig. 9, 11) (Biever et al., 2020), have either a high overlap with the FMRP-Clipped data or the subsets that overlapped with FMRP-Clipped data drove the wide differences when FMRP is lost. This is most striking when examining the mRNAs represent SFARI genes, where both SFARI genes that are mapped by FMRP or not clipped by FMRP are equally enriched in RNA Granules, but only SFARI genes that are clipped by FMRP are affected by the loss of FMRP (Fig. 13). In other words, the elimination of FMRP does alter the abundances of FMRP-Clipped mRNAs in the RNA Granules, but not drastic enough to change the enrichment of FMRP-Clipped mRNAs in the granules.

Together, our finding suggests that FMRP might serve other roles to stalled ribosomes. One possibility is FMRP serves as an overall stabilizer for the RNA granules, specifically for the mRNAs clipped by FMRP. FMRP contains RGG low complexity domain that allows phase separation to form spontaneously (Tsang et al., 2019; Zhang et al., 2022). This may explain how FMRP is associated to the liquid-liquid phase separated granules in neurites (Graber et al., 2013) and increased mGluR-LTD when lost (Huber et al., 2002; Hou et al., 2006). However, this indicates that the loss of FMRP should reduce the numbers of RNA Granules we observed in our samples since the loss of FMRP should cause RNA Granules to be vulnerable. Instead, we observed, if anything, an increase in the number of ribosomes in RG (Fig 1D, 1H), which implies this hypothesis to be unlikely. Another possibility is FMRP is crucial for the overall reactivation of the ribosomes. FMRP is subjugated to post translational modification by neuronal stimulus such as mGluR-LTD. Moreover, a study had reported that sumoylation of FMRP is crucial for its detachment from the dendritic granules (Khayachi et al., 2018). In other words, there is a

possibility that the modification of FMRP serves as a switch for the dissolution of RNA Granules to resume its translation. However, an issue with this hypothesis is that it does not explain how and why the subset of mRNA, such as FMRP-Clipped mRNA, are associated to the FMRP and not the others. Lastly, FMRP may play no role in stalled ribosomes. Afterall, some study had suggested FMR1-KO phenotypes can be rescued by restoring the initiation pathway (Santini et al., 2017; Hooshmandi et al., 2023). Our own results also suggested that the loss of FMRP altered the mTOR pathway (Fig 11D). Yet, this hypothesis does not explain how or why FMRP is highly associated to our granules. More investigations are required to determine the role of FMRP in stalled ribosomes.

The results from WT RG were generally comparable to rat RG, for both the cellular level magnesium group and high magnesium group. In addition, we also showed magnesium level does not alter the state of the ribosomes in RC through Cryo-EM (Fig 4a). Together, these data suggested that even though cellular level  $Mg^{2+}$  may destabilize yeast and bacterial ribosomes (Bhattacharya et al., 2010; Yu et al., 2023), it did not fractionate neuronal ribosomes. The only surprising discrepancy between the high  $Mg^{2+}$  group and the cellular level  $Mg^{2+}$  group was with the significant decrease in secretory proteins (Fig. 4b). Secretory proteins are the proteins synthesized by the ER. Since we are trying to extract RNA granules that were already transported out to the neurites, the presence of secretory proteins was seen as contamination. Thus, high magnesium samples were recognized to be superior for us. Yet, how the increase of magnesium led to reduction of secretory proteins was unclear. On the other hand, the Cryo-EM result (Fig 4a) also showed that the ribosome clusters mainly contain stalled ribosomes with high levels of ribosomes in the A/P and P/E hybrid state whether the magnesium level is high or low. Thus, the only major distinction between the two fractions is FMRP related mRNAs (Fig 6E) (Anadolu et

al., 2023). Yet, the reasons why FMRP associated strongly with RNA Granules and not ribosome clusters and how FMRP-Clipped sequences were more enriched in RNA Granules remains a mystery. These are some important questions to answer the differences between RNA Granules and ribosomal clusters.

Unlike the previous results where both the monosomes and polysomes mRNA were enriched in the rat RG (Anadolu et al., 2023), our sequencing result suggested that stalled ribosomes contain mostly monosomes and not polysomes (Fig 8). Previously, monosomes have been reported to be crucial for local protein synthesis (Biever et al., 2020). Thus, this finding supports the idea that stalled ribosomes are a mechanism involved in local protein synthesis. The idea that stalled ribosomes are monosomes is consistent with the finding that mRNAs are stalled near the beginning of the transcript (Anadolu et al., 2023). Thus, once stalling sequences are recognized by the stalled ribosomes, the monosomes are packaged. Moreover, if most ribosomes are tied up in stalled monosomes, initiation would be slowed, and this would also lead to more monosome-mediated translation in neurons. In addition, the proposition that stalled ribosomes are monosomes is consistent with the hypothesis that many synapses only retain low copy of proteins (Biever et al., 2019). Therefore, the reactivation of monosomes translation would be sufficient for local proteome. Thus, we propose that monosomes serve as the dominant translational machinery for stalled ribosomes.

However, if monosomes are the main translator, then what caused the clustering of the ribosomes in the RNA Granules (Anadolu et al., 2023)? Our unpublished data of the Cryo-EM showed many 60S ribosomes associated to the ribosome clusters, suggesting that 60S-60S interactions underlie clusters. However, this does not answer why the clustering was broken up by nuclease. Another hypothesis is that the noncoding RNAs lead to the clustering of the

ribosomes. Despite high nuclease treatments, we still observed longer than 35nts RPFs in our samples, and these longer mRNAs are later identified to be noncoding mRNAs. Certain noncoding RNAs, such as the snoRNAs, serve an important role for rRNA modification (Bratkovic et al, 2020). A subset of these snoRNAs is also particular to neurons (Bratkovic et al, 2020). Thus, snoRNAs might be the factor that had caused the accumulation of ribosomes subunit onto the monosomes and results in the clustering of the ribosomes from the previous TEM images (Anadolu et al., 2023). Perhaps, snoRNAs might act as the stabilizer for the clustering of the ribosomes. In addition, it has been reported that unlike the polysomes fraction, RNA Granules are insensitive to EGTA addition (El Fatimy et al, 2016). EGTA is a chelating agent that disrupts the protein-protein or protein-RNA interactions that are reliant to ion stabilization (Nörtemann, 1999). Thus, what is holding the monosomes in the clustering of the RG might be independent of metal ion interactions. This fits our model that snoRNAs cause the clustering, since ribosomal interaction with the mRNAs are heavily reliant on metal ions (Akanuma, 2021). It would be interesting to explore if the 60S ribosomes or the noncoding RNA drove the clustering.

Our HOMER motif analysis did not completely replicate previous results from rat RNA Granules (Fig 14C) (Anadolu et al., 2023) in individual groups. We suspect the issue might lie in HOMER analysis. During HOMER Analysis, the computer program conducts a global search for motifs and then allows mismatch in the short search sequence to increase sensitivity (HOMER motif analysis, n.d.). Thus, there is a possibility that the original WGA motif enrichment was created through the mismatch step. Thus, HOMER Analysis might not be the most reliable way to predict the stalling sequence. Our unpublished work using machine learning to predict stalling sequences indicated that there are two independent sites underlying stalling –

one encoding the peptide sequence of the nascent chain, and one encoding the mRNAs near the exit channel. A major future direction is to better define the stalling sites and perhaps this will distinguish sites that are regulated by FMRP, and other stalling sites that are not. Nevertheless, most peaks appear to be present in the absence of FMRP and thus most ribosome stalling in neurons is not dependent on FMRP.

## **References**

- Akanuma, G. (2021). Diverse relationships between metal ions and the ribosome. *Bioscience, Biotechnology, and Biochemistry*, 85(7), 1582–1593. <https://doi.org/10.1093/bbb/zbab070>
- Amorim, I. S., Kedia, S., Kouloulia, S., Simbriger, K., Gantois, I., Jafarnejad, S. M., Li, Y., Kampaite, A., Pooters, T., Romanò, N., & Gkogkas, C. G. (2018). Loss of eIF4E Phosphorylation Engenders Depression-like Behaviors via Selective mRNA Translation. *Journal of Neuroscience*, 38(8), 2118–2133. <https://doi.org/10.1523/JNEUROSCI.2673-17.2018>
- Anadolu, M. N., Sun, J., Kailasam, S., Chalkiadaki, K., Krimbacher, K., Li, J. T.-Y., Markova, T., Jafarnejad, S. M., Lefebvre, F., Ortega, J., Gkogkas, C. G., & Sossin, W. S. (2023). Ribosomes in RNA Granules Are Stalled on mRNA Sequences That Are Consensus Sites for FMRP Association. *The Journal of Neuroscience*, 43(14), 2440–2459. <https://doi.org/10.1523/JNEUROSCI.1002-22.2023>
- Anadolu, M. N., Sun, J., Li, J. T.-Y., Graber, T. E., Ortega, J., & Sossin, W. S. (2024). Puromycin reveals a distinct conformation of neuronal ribosomes. *The Journal of Neuroscience*, 121(7) <https://doi.org/10.1073/pnas.2306993121>
- Anderson, B. R., Chopra, P., Suhl, J. A., Warren, S. T., & Bassell, G. J. (2016). Identification of consensus binding sites clarifies FMRP binding determinants. *Nucleic Acids Research*, 44(14), 6649–6659. <https://doi.org/10.1093/nar/gkw593>
- Ascano, M., Mukherjee, N., Bandaru, P., Miller, J. B., Nusbaum, J. D., Corcoran, D. L., Langlois, C., Munschauer, M., Dewell, S., Hafner, M., Williams, Z., Ohler, U., & Tuschl, T. (2012). FMRP targets distinct mRNA sequence elements to regulate protein expression. *Nature*, 492(7429), 382–386. <https://doi.org/10.1038/nature11737>
- Aschrafi, A., Cunningham, B. A., Edelman, G. M., & Vanderklish, P. W. (2005). The fragile X mental retardation protein and group I metabotropic glutamate receptors regulate levels of mRNA

granules in brain. *Proceedings of the National Academy of Sciences*, 102(6), 2180–2185.  
<https://doi.org/10.1073/pnas.0409803102>

Aviner, R. (2020). The science of puromycin: From studies of ribosome function to applications in biotechnology. *Computational and Structural Biotechnology Journal*, 18, 1074–1083.  
<https://doi.org/10.1016/j.csbj.2020.04.014>

Bagni, C., Mannucci, L., Dotti, C. G., & Amaldi, F. (2000). Chemical Stimulation of Synaptosomes Modulates  $\alpha$ -Ca<sup>2+</sup>/Calmodulin-Dependent Protein Kinase II mRNA Association to Polysomes. *The Journal of Neuroscience*, 20(10), RC76–RC76.  
<https://doi.org/10.1523/JNEUROSCI.20-10-j0004.2000>

Bakker, C. e., Kooy, R. f., D’Hooge, R., Tamanini, F., Willemsen, R., Nieuwenhuizen, I., De Vries, B. b. a., Reyniers, E., Hoogeveen, A. t., Willems, P. j., De Deyn, P. p., & Oostra, B. a. (2000). Introduction of a FMR1 transgene in the fragile X knockout mouse. *Neuroscience Research Communications*, 26(3), 265–277. [https://doi.org/10.1002/1520-6769\(200005/06\)26:3<265::AID-NRC13>3.0.CO;2-T](https://doi.org/10.1002/1520-6769(200005/06)26:3<265::AID-NRC13>3.0.CO;2-T)

Baltaci, S. B., Mogulkoc, R., & Baltaci, A. K. (2019). Molecular Mechanisms of Early and Late LTP. *Neurochemical Research*, 44(2), 281–296. <https://doi.org/10.1007/s11064-018-2695-4>

Banko, J. L., Poulin, F., Hou, L., DeMaria, C. T., Sonenberg, N., & Klann, E. (2005). The Translation Repressor 4E-BP2 Is Critical for eIF4F Complex Formation, Synaptic Plasticity, and Memory in the Hippocampus. *Journal of Neuroscience*, 25(42), 9581–9590.  
<https://doi.org/10.1523/JNEUROSCI.2423-05.2005>

Bhattacharya, A., McIntosh, K. B., Willis, I. M., & Warner, J. R. (2010). Why Dom34 Stimulates Growth of Cells with Defects of 40S Ribosomal Subunit Biosynthesis. *Molecular and Cellular Biology*, 30(23), 5562–5571. <https://doi.org/10.1128/MCB.00618-10>

Biever, A., Doulin-Asp, P. G., Shuman, E. M. (2019) Local Translation in Neuronal Processes. *Current Opinion in Neurobiology*, 57, 141-148. <https://doi.org/10.1016/j.conb.2019.02.008>.

Biever, A., Glock, C., Tushev, G., Ciirdaeva, E., Dalmay, T., Langer, J. D., & Schuman, E. M. (2020). Monosomes actively translate synaptic mRNAs in neuronal processes. *Science*, 367(6477). <https://doi.org/10.1126/science.aay4991>

Bonni, A., Brunet, A., West, A. E., Datta, S. R., Takasu, M. A., & Greenberg, M. E. (1999). Cell Survival Promoted by the Ras-MAPK Signaling Pathway by Transcription-Dependent and -Independent Mechanisms. *Science*, 286(5443), 1358–1362.  
<https://doi.org/10.1126/science.286.5443.1358>

Bramham, C. R., & Messaoudi, E. (2005). BDNF function in adult synaptic plasticity: The synaptic consolidation hypothesis. *Progress in Neurobiology*, 76(2), 99–125.  
<https://doi.org/10.1016/j.pneurobio.2005.06.003>

- Bratkovič, T., Božič, J., & Rogelj, B. (2020). Functional diversity of small nucleolar RNAs. *Nucleic Acids Research*, 48(4), 1627–1651. <https://doi.org/10.1093/nar/gkz1140>
- Buffington, S. A., Huang, W., & Costa-Mattioli, M. (2014). Translational control in synaptic plasticity and cognitive dysfunction. *Annual Review of Neuroscience*, 37, 17–38. <https://doi.org/10.1146/annurev-neuro-071013-014100>
- Caccamo, A., Branca, C., Talboom, J. S., Shaw, D. M., Turner, D., Ma, L., Messina, A., Huang, Z., Wu, J., & Oddo, S. (2015). Reducing Ribosomal Protein S6 Kinase 1 Expression Improves Spatial Memory and Synaptic Plasticity in a Mouse Model of Alzheimer's Disease. *The Journal of Neuroscience*, 35(41), 14042–14056. <https://doi.org/10.1523/JNEUROSCI.2781-15.2015>
- Cajigas, I. J., Will, T., & Schuman, E. M. (2010). Protein homeostasis and synaptic plasticity. *The EMBO Journal*, 29(16), 2746–2752. <https://doi.org/10.1038/emboj.2010.173>
- Cajigas, I. J., Tushev, G., Will, T. J., tom Dieck, S., Fuerst, N., & Schuman, E. M. (2012). The local transcriptome in the synaptic neuropil revealed by deep sequencing and high-resolution imaging. *Neuron*, 74(3), 453–466. <https://doi.org/10.1016/j.neuron.2012.02.036>
- Campbell, D. S., & Holt, C. E. (2001). Chemotropic responses of retinal growth cones mediated by rapid local protein synthesis and degradation. *Neuron*, 32(6), 1013–1026. [https://doi.org/10.1016/s0896-6273\(01\)00551-7](https://doi.org/10.1016/s0896-6273(01)00551-7)
- Carroll, M., Warren, O., Fan, X., Sossin, W. (2004) 5-HT stimulates eEF2 dephosphorylation in a rapamycin-sensitive manner in Aplysia neurites. *Journal of Neurochemistry*. 90(6), 1464-1476. <https://doi.org/10.1111/j.1471-4159.2004.02634.x>
- Ceman, S., O'Donnell, W. T., Reed, M., Patton, S., Pohl, J., & Warren, S. T. (2003). Phosphorylation influences the translation state of FMRP-associated polyribosomes. *Human Molecular Genetics*, 12(24), 3295–3305. <https://doi.org/10.1093/hmg/ddg350>
- Cheever, A., & Ceman, S. (2009). Translation regulation of mRNAs by the fragile X family of proteins through the miRNA pathway. *RNA Biology*, 6(2), 175–178.
- Cohen, L. D., Zuchman, R., Sorokina, O., Müller, A., Dieterich, D. C., Armstrong, J. D., Ziv, T., & Ziv, N. E. (2013). Metabolic Turnover of Synaptic Proteins: Kinetics, Interdependencies and Implications for Synaptic Maintenance. *PLOS ONE*, 8(5), e63191. <https://doi.org/10.1371/journal.pone.0063191>
- Costa-Mattioli, M., Gobert, D., Harding, H., Herdy, B., Azzi, M., Bruno, M., Bidinosti, M., Ben Mamou, C., Marcinkiewicz, E., Yoshida, M., Imataka, H., Cuello, A. C., Seidah, N., Sossin, W., Lacaille, J.-C., Ron, D., Nader, K., & Sonenberg, N. (2005). Translational control of hippocampal synaptic plasticity and memory by the eIF2alpha kinase GCN2. *Nature*, 436(7054), 1166–1173. <https://doi.org/10.1038/nature03897>

- Costa-Mattioli, M., Sossin, W. S., Klann, E., & Sonenberg, N. (2009). Translational Control of Long-Lasting Synaptic Plasticity and Memory. *Neuron*, *61*(1), 10–26. <https://doi.org/10.1016/j.neuron.2008.10.055>
- Darnell, J. C., Van Driesche, S. J., Zhang, C., Hung, K. Y. S., Mele, A., Fraser, C. E., Stone, E. F., Chen, C., Fak, J. J., Chi, S. W., Licatalosi, D. D., Richter, J. D., & Darnell, R. B. (2011). FMRP stalls ribosomal translocation on mRNAs linked to synaptic function and autism. *Cell*, *146*(2), 247–261. <https://doi.org/10.1016/j.cell.2011.06.013>
- Davidkova, G., & Carroll, R. C. (2007). Characterization of the role of microtubule-associated protein 1B in metabotropic glutamate receptor-mediated endocytosis of AMPA receptors in hippocampus. *The Journal of Neuroscience: The Official Journal of the Society for Neuroscience*, *27*(48), 13273–13278. <https://doi.org/10.1523/JNEUROSCI.3334-07.2007>
- Debanne, D., Campanac, E., Bialowas, A., Carlier, E., & Alcaraz, G. (2011). Axon physiology. *Physiological Reviews*, *91*(2), 555–602. <https://doi.org/10.1152/physrev.00048.2009>
- Deng, P.-Y., & Klyachko, V. A. (2021). Channelopathies in fragile X syndrome. *Nature Reviews. Neuroscience*, *22*(5), 275–289. <https://doi.org/10.1038/s41583-021-00445-9>
- Dever, T. E., Dinman, J. D., & Green, R. (2018). Translation Elongation and Recoding in Eukaryotes. *Cold Spring Harbor Perspectives in Biology*, *10*(8), a032649. <https://doi.org/10.1101/cshperspect.a032649>
- Di Prisco, G. V., Huang, W., Buffington, S. A., Hsu, C.-C., Bonnen, P. E., Placzek, A. N., Sidrauski, C., Krnjević, K., Kaufman, R. J., Walter, P., & Costa-Mattioli, M. (2014). Translational control of mGluR-dependent long-term depression and object-place learning by eIF2 $\alpha$ . *Nature Neuroscience*, *17*(8), 1073–1082. <https://doi.org/10.1038/nn.3754>
- Dörrbaum, A. R., Kochen, L., Langer, J. D., & Schuman, E. M. (2018). Local and global influences on protein turnover in neurons and glia. *eLife*, *7*, e34202. <https://doi.org/10.7554/eLife.34202>
- Douka, K., Agapiou, M., Birds, I., & Aspden, J. L. (2021). Optimization of Ribosome Footprinting Conditions for Ribo-Seq in Human and Drosophila melanogaster Tissue Culture Cells. *Frontiers in Molecular Biosciences*, *8*, 791455. <https://doi.org/10.3389/fmolb.2021.791455>
- Ekholm, R., & Hydén, H. (1965). Polysomes from microdissected fresh neurons. *Journal of Ultrastructure Research*, *13*(3), 269–280. [https://doi.org/10.1016/S0022-5320\(65\)80076-4](https://doi.org/10.1016/S0022-5320(65)80076-4)
- El Fatimy, R., Davidovic, L., Tremblay, S., Jaglin, X., Dury, A., Robert, C., De Koninck, P., & Khandjian, E. W. (2016). Tracking the Fragile X Mental Retardation Protein in a Highly Ordered Neuronal RiboNucleoParticles Population: A Link between Stalled Polyribosomes and RNA Granules. *PLoS Genetics*, *12*(7), e1006192. <https://doi.org/10.1371/journal.pgen.1006192>

Elvira, G., Wasiak, S., Blandford, V., Tong, X.-K., Serrano, A., Fan, X., Sánchez-Carbente, M. del R., Servant, F., Bell, A. W., Boismenu, D., Lacaille, J.-C., McPherson, P. S., DesGroseillers, L., & Sossin, W. S. (2006). Characterization of an RNA Granule from Developing Brain \*. *Molecular & Cellular Proteomics*, 5(4), 635–651. <https://doi.org/10.1074/mcp.M500255-MCP200>

Enam, S. U., Zinshteyn, B., Goldman, D. H., Cassani, M., Livingston, N. M., Seydoux, G., & Green, R. (2020). Puromycin reactivity does not accurately localize translation at the subcellular level. *eLife*, 9, e60303. <https://doi.org/10.7554/eLife.60303>

Ferron, L. (2016). Fragile X mental retardation protein controls ion channel expression and activity. *The Journal of Physiology*, 594(20), 5861–5867. <https://doi.org/10.1113/JP270675>

Garreau de Loubresse, N., Prokhorova, I., Holtkamp, W., Rodnina, M. V., Yusupova, G., & Yusupov, M. (2014). Structural basis for the inhibition of the eukaryotic ribosome. *Nature*, 513(7519), 517–522. <https://doi.org/10.1038/nature13737>

Glinicy, N. J., & Ingolia, N. T. (2017). Transcriptome-wide measurement of translation by ribosome profiling. *Methods*, 126, 112–129. <https://doi.org/10.1016/j.ymeth.2017.05.028>

Graber, T. E., Hébert-Seropian, S., Khoutorsky, A., David, A., Yewdell, J. W., Lacaille, J.-C., & Sossin, W. S. (2013). Reactivation of stalled polyribosomes in synaptic plasticity. *Proceedings of the National Academy of Sciences*, 110(40), 16205–16210. <https://doi.org/10.1073/pnas.1307747110>

Graber, T. E., Freemantle, E., Anadolu, M. N., Hébert-Seropian, S., MacAdam, R. L., Shin, U., Hoang, H.-D., Alain, T., Lacaille, J.-C., & Sossin, W. S. (2017). UPF1 Governs Synaptic Plasticity through Association with a STAU2 RNA Granule. *Journal of Neuroscience*, 37(38), 9116–9131. <https://doi.org/10.1523/JNEUROSCI.0088-17.2017>

Gross, C., Yao, X., Pong, D. L., Jeromin, A., & Bassell, G. J. (2011). Fragile X Mental Retardation Protein Regulates Protein Expression and mRNA Translation of the Potassium Channel Kv4.2. *Journal of Neuroscience*, 31(15), 5693–5698. <https://doi.org/10.1523/JNEUROSCI.6661-10.2011>

Guzowski, J. F., Lyford, G. L., Stevenson, G. D., Houston, F. P., McGaugh, J. L., Worley, P. F., & Barnes, C. A. (2000). Inhibition of Activity-Dependent Arc Protein Expression in the Rat Hippocampus Impairs the Maintenance of Long-Term Potentiation and the Consolidation of Long-Term Memory. *Journal of Neuroscience*, 20(11), 3993–4001. <https://doi.org/10.1523/JNEUROSCI.20-11-03993.2000>

Hansen, J. L., Moore, P. B., & Steitz, T. A. (2003). Structures of Five Antibiotics Bound at the Peptidyl Transferase Center of the Large Ribosomal Subunit. *Journal of Molecular Biology*, 330(5), 1061–1075. [https://doi.org/10.1016/S0022-2836\(03\)00668-5](https://doi.org/10.1016/S0022-2836(03)00668-5)

Heyer, E. E., & Moore, M. J. (2016). Redefining the Translational Status of 80S Monosomes. *Cell*, 164(4), 757–769. <https://doi.org/10.1016/j.cell.2016.01.003>

Heinz, S., Benner, C., Spann, N., Bertolino, E., Lin, Y. C., Laslo, P., Cheng, J. X., Murre, C., Singh, H., & Glass, C. K. (2010). Simple combinations of lineage-determining transcription factors prime cis-regulatory elements required for macrophage and B cell identities. *Molecular Cell*, 38(4), 576–589. <https://doi.org/10.1016/j.molcel.2010.05.004>

Hobson, B. D., Kong, L., Hartwick, E. W., Gonzalez, R. L., & Sims, P. A. (2020). Elongation inhibitors do not prevent the release of puromycylated nascent polypeptide chains from ribosomes. *eLife*, 9, e60048. <https://doi.org/10.7554/eLife.60048>

Hoeffler, C. A., & Klann, E. (2010). mTOR signaling: At the crossroads of plasticity, memory and disease. *Trends in Neurosciences*, 33(2), 67–75. <https://doi.org/10.1016/j.tins.2009.11.003>

Homer Motif Analysis (n.d.). UCSD. <http://homer.ucsd.edu/homer/motif/>

Hooshmandi, M., Sharma, V., Thörn Perez, C., Sood, R., Krimbacher, K., Wong, C., Lister, K. C., Ureña Guzmán, A., Bartley, T. D., Rocha, C., Maussion, G., Nadler, E., Roque, P. M., Gantois, I., Popic, J., Lévesque, M., Kaufman, R. J., Avoli, M., Sanz, E., ... Khoutorsky, A. (2023). Excitatory neuron-specific suppression of the integrated stress response contributes to autism-related phenotypes in fragile X syndrome. *Neuron*, 111(19), 3028-3040.e6. <https://doi.org/10.1016/j.neuron.2023.06.017>

Hou, L., & Klann, E. (2004). Activation of the phosphoinositide 3-kinase-Akt-mammalian target of rapamycin signaling pathway is required for metabotropic glutamate receptor-dependent long-term depression. *The Journal of Neuroscience: The Official Journal of the Society for Neuroscience*, 24(28), 6352–6361. <https://doi.org/10.1523/JNEUROSCI.0995-04.2004>

Hou, L., Antion, M. D., Hu, D., Spencer, C. M., Paylor, R., & Klann, E. (2006). Dynamic translational and proteasomal regulation of fragile X mental retardation protein controls mGluR-dependent long-term depression. *Neuron*, 51(4), 441–454. <https://doi.org/10.1016/j.neuron.2006.07.005>

Huber, K. M., Kayser, M. S., & Bear, M. F. (2000). Role for Rapid Dendritic Protein Synthesis in Hippocampal mGluR-Dependent Long-Term Depression. *Science*, 288(5469), 1254–1256. <https://doi.org/10.1126/science.288.5469.1254>

Huber, K. M., Gallagher, S. M., Warren, S. T., & Bear, M. F. (2002). Altered synaptic plasticity in a mouse model of fragile X mental retardation. *Proceedings of the National Academy of Sciences*, 99(11), 7746–7750. <https://doi.org/10.1073/pnas.122205699>

Ingolia, N. T., Brar, G. A., Rouskin, S., McGeachy, A. M., & Weissman, J. S. (2012). The ribosome profiling strategy for monitoring translation in vivo by deep sequencing of ribosome-

protected mRNA fragments. *Nature Protocols*, 7(8), Article 8.  
<https://doi.org/10.1038/nprot.2012.086>

Ingolia, N. T. (2014). Ribosome profiling: New views of translation, from single codons to genome scale. *Nature Reviews Genetics*, 15(3), 205–213. <https://doi.org/10.1038/nrg3645>

Ishizuka, N., Cowan, W. M., & Amaral, D. G. (1995). A quantitative analysis of the dendritic organization of pyramidal cells in the rat hippocampus. *The Journal of Comparative Neurology*, 362(1), 17–45. <https://doi.org/10.1002/cne.903620103>

Jung, H., Gkogkas, C. G., Sonenberg, N., & Holt, C. E. (2014). Remote control of gene function by local translation. *Cell*, 157(1), 26–40. <https://doi.org/10.1016/j.cell.2014.03.005>

Kanai, Y., Dohmae, N., & Hirokawa, N. (2004). Kinesin transports RNA: Isolation and characterization of an RNA-transporting granule. *Neuron*, 43(4), 513–525.  
<https://doi.org/10.1016/j.neuron.2004.07.022>

Kelen, K. V. D., Beyaert, R., Inzé, D., & Veylder, L. D. (2009). Translational control of eukaryotic gene expression. *Critical Reviews in Biochemistry and Molecular Biology*, 44(4), 143–168. <https://doi.org/10.1080/10409230902882090>

Kenney, J. W., Genheden, M., Moon, K.-M., Wang, X., Foster, L. J., & Proud, C. G. (2016). Eukaryotic elongation factor 2 kinase regulates the synthesis of microtubule-related proteins in neurons. *Journal of Neurochemistry*, 136(2), 276–284. <https://doi.org/10.1111/jnc.13407>

Khayachi, A., Gwizdek, C., Poupon, G., Alcor, D., Chafai, M., Cassé, F., Maurin, T., Prieto, M., Folci, A., De Graeve, F., Castagnola, S., Gautier, R., Schorova, L., Loriol, C., Pronot, M., Besse, F., Brau, F., Deval, E., Bardoni, B., & Martin, S. (2018). Sumoylation regulates FMRP-mediated dendritic spine elimination and maturation. *Nature Communications*, 9(1), 757.  
<https://doi.org/10.1038/s41467-018-03222-y>

Kipper, K., Mansour, A., & Pulk, A. (2022). Neuronal RNA granules are ribosome complexes stalled at the pre-translocation state. *Journal of Molecular Biology*, 434(20), 167801.  
<https://doi.org/10.1016/j.jmb.2022.167801>

Kraushar, M. L., Krupp, F., Harnett, D., Turko, P., Ambrozkiwicz, M. C., Sprink, T., Imami, K., Günningmann, M., Zinnall, U., Vieira-Vieira, C. H., Schaub, T., Münster-Wandowski, A., Bürger, J., Borisova, E., Yamamoto, H., Rasin, M.-R., Ohler, U., Beule, D., Mielke, T., ... Spahn, C. M. T. (2021). Protein Synthesis in the Developing Neocortex at Near-Atomic Resolution Reveals Ebp1-Mediated Neuronal Proteostasis at the 60S Tunnel Exit. *Molecular Cell*, 81(2), 304-322.e16. <https://doi.org/10.1016/j.molcel.2020.11.037>

Krichevsky, A. M., & Kosik, K. S. (2001). Neuronal RNA Granules: A Link between RNA Localization and Stimulation-Dependent Translation. *Neuron*, 32(4), 683–696.  
[https://doi.org/10.1016/S0896-6273\(01\)00508-6](https://doi.org/10.1016/S0896-6273(01)00508-6)

- Kurosaki, T., Mitsutomi, S., Hewko, A., Akimitsu, N., & Maquat, L. E. (2022). Integrative omics indicate FMRP sequesters mRNA from translation and deadenylation in human neuronal cells. *Molecular Cell*, 82(23), 4564-4581.e11. <https://doi.org/10.1016/j.molcel.2022.10.018>
- Langille, J. J., Ginzberg, K., & Sossin, W. S. (2019). Polysomes identified by live imaging of nascent peptides are stalled in hippocampal and cortical neurites. *Learning & Memory*, 26(9), 351–362. <https://doi.org/10.1101/lm.049965.119>
- Lai, A., Valdez-Sinon, A. N., & Bassell, G. J. (2020). Regulation of RNA granules by FMRP and implications for neurological diseases. *Traffic*, 21(7), 454–462. <https://doi.org/10.1111/tra.12733>
- Liao, Y., Smyth, G. K., & Shi, W. (2014). featureCounts: An efficient general purpose program for assigning sequence reads to genomic features. *Bioinformatics*, 30(7), 923–930. <https://doi.org/10.1093/bioinformatics/btt656>
- Liu, B., & Qian, S.-B. (2016). Characterizing inactive ribosomes in translational profiling. *Translation*, 4(1), e1138018. <https://doi.org/10.1080/21690731.2015.1138018>
- Lüscher, C., & Huber, K. (2010). Group 1 mGluR-dependent synaptic long-term depression: Mechanisms and implications for circuitry and disease. *Neuron*, 65(4). <https://doi.org/10.1016/j.neuron.2010.01.016>
- Ma, T. (2021). Roles of Eukaryotic Elongation Factor 2 Kinase (eEF2K) in Neuronal Plasticity, Cognition, and Alzheimer Disease. *Journal of Neurochemistry*, 166(1), 47-57. <https://doi.org/10.1111/jnc.15541>
- Masek, T., del Llano, E., Gahurova, L., Kubelka, M., Susor, A., Roucova, K., Lin, C.-J., Bruce, A. W., & Pospisek, M. (2020). Identifying the Translatome of Mouse NEBD-Stage Oocytes via SSP-Profilng; A Novel Polysome Fractionation Method. *International Journal of Molecular Sciences*, 21(4), Article 4. <https://doi.org/10.3390/ijms21041254>
- Maurin, T., Lebrigand, K., Castagnola, S., Paquet, A., Jarjat, M., Popa, A., Grossi, M., Rage, F., & Bardoni, B. (2018). HITS-CLIP in various brain areas reveals new targets and new modalities of RNA binding by fragile X mental retardation protein. *Nucleic Acids Research*, 46(12), 6344–6355. <https://doi.org/10.1093/nar/gky267>
- Mei, F., Nagappan, G., Ke, Y., Sacktor, T. C., & Lu, B. (2011). BDNF Facilitates L-LTP Maintenance in the Absence of Protein Synthesis through PKM $\zeta$ . *PLoS ONE*, 6(6), e21568. <https://doi.org/10.1371/journal.pone.0021568>
- Martin, M. (2011). Cutadapt removes adapter sequences from high-throughput sequencing reads. *EMBnet.Journal*, 17(1), Article 1. <https://doi.org/10.14806/ej.17.1.200>

- Muslimov, I. A., Nimmrich, V., Hernandez, A. I., Tcherepanov, A., Sacktor, T. C., & Tiedge, H. (2004). Dendritic Transport and Localization of Protein Kinase M $\zeta$  mRNA. *Journal of Biological Chemistry*, 279(50), 52613–52622. <https://doi.org/10.1074/jbc.M409240200>
- Nalavadi, V. C., Muddashetty, R. S., Gross, C., & Bassell, G. J. (2012). Dephosphorylation-induced ubiquitination and degradation of FMRP in dendrites: A role in immediate early mGluR-stimulated translation. *The Journal of Neuroscience: The Official Journal of the Society for Neuroscience*, 32(8), 2582–2587. <https://doi.org/10.1523/JNEUROSCI.5057-11.2012>
- Napoli, I., Mercaldo, V., Boyl, P. P., Eleuteri, B., Zalfa, F., De Rubeis, S., Di Marino, D., Mohr, E., Massimi, M., Falconi, M., Witke, W., Costa-Mattioli, M., Sonenberg, N., Achsel, T., & Bagni, C. (2008). The fragile X syndrome protein represses activity-dependent translation through CYFIP1, a new 4E-BP. *Cell*, 134(6), 1042–1054. <https://doi.org/10.1016/j.cell.2008.07.031>
- Narayanan, U., Nalavadi, V., Nakamoto, M., Pallas, D. C., Ceman, S., Bassell, G. J., & Warren, S. T. (2007). FMRP phosphorylation reveals an immediate-early signaling pathway triggered by group I mGluR and mediated by PP2A. *The Journal of Neuroscience: The Official Journal of the Society for Neuroscience*, 27(52), 14349–14357. <https://doi.org/10.1523/JNEUROSCI.2969-07.2007>
- Niere, F., Wilkerson, J. R., & Huber, K. M. (2012). Evidence for a Fragile X Mental Retardation Protein-Mediated Translational Switch in Metabotropic Glutamate Receptor-Triggered Arc Translation and Long-Term Depression. *Journal of Neuroscience*, 32(17), 5924–5936. <https://doi.org/10.1523/JNEUROSCI.4650-11.2012>
- Nörtemann, B. (1999). Biodegradation of EDTA. *Applied Microbiology and Biotechnology*, 51(6), 751–759. <https://doi.org/10.1007/s002530051458>
- Nosyreva, E. D., & Huber, K. M. (2006). Metabotropic Receptor-Dependent Long-Term Depression Persists in the Absence of Protein Synthesis in the Mouse Model of Fragile X Syndrome. *Journal of Neurophysiology*, 95(5), 3291–3295. <https://doi.org/10.1152/jn.01316.2005>
- Park, S., Park, J. M., Kim, S., Kim, J.-A., Shepherd, J. D., Smith-Hicks, C. L., Chowdhury, S., Kaufmann, W., Kuhl, D., Ryazanov, A. G., Haganir, R. L., Linden, D. J., & Worley, P. F. (2008). Elongation Factor 2 and Fragile X Mental Retardation Protein Control the Dynamic Translation of Arc/Arg3.1 Essential for mGluR-LTD. *Neuron*, 59(1), 70–83. <https://doi.org/10.1016/j.neuron.2008.05.023>
- Popper, B., Bürkle, M., Ciccopiedi, G., Marchioretto, M., Forné, I., Imhof, A., Straub, T., Viero, G., Götz, M., & Schieweck, R. (2024). Ribosome inactivation regulates translation elongation in neurons. *Journal of Biological Chemistry*, 300(2), 105648. <https://doi.org/10.1016/j.jbc.2024.105648>

Richter, J. D., & Zhao, X. (2021). The molecular biology of FMRP: New insights into fragile X syndrome. *Nature Reviews. Neuroscience*, 22(4), 209–222. <https://doi.org/10.1038/s41583-021-00432-0>

Risebrough, R. W., Tissières, A., & Watson, J. D. (1962). Messenger-rna attachment to active ribosomes. *Proceedings of the National Academy of Sciences*, 48(3), 430–436. <https://doi.org/10.1073/pnas.48.3.430>

Robinson, M. D., McCarthy, D. J., & Smyth, G. K. (2010). edgeR: A Bioconductor package for differential expression analysis of digital gene expression data. *Bioinformatics*, 26(1), 139–140. <https://doi.org/10.1093/bioinformatics/btp616>

Santini, E., Huynh, T. N., Longo, F., Koo, S. Y., Mojica, E., D'Andrea, L., Bagni, C., & Klann, E. (2017). Reducing eIF4E-eIF4G interactions restores the balance between protein synthesis and actin dynamics in fragile X syndrome model mice. *Science Signaling*, 10(504), ean0665. <https://doi.org/10.1126/scisignal.aan0665>

Serafini, T., Kennedy, T. E., Galko, M. J., Mirzayan, C., Jessell, T. M., & Tessier-Lavigne, M. (1994). The netrins define a family of axon outgrowth-promoting proteins homologous to *C. elegans* UNC-6. *Cell*, 78(3), 409–424. [https://doi.org/10.1016/0092-8674\(94\)90420-0](https://doi.org/10.1016/0092-8674(94)90420-0)

Shah, S., Molinaro, G., Liu, B., Wang, R., Huber, K. M., & Richter, J. D. (2020). FMRP Control of Ribosome Translocation Promotes Chromatin Modifications and Alternative Splicing of Neuronal Genes Linked to Autism. *Cell Reports*, 30(13), 4459-4472.e6. <https://doi.org/10.1016/j.celrep.2020.02.076>

Shenvi, C. L., Dong, K. C., Friedman, E. M., Hanson, J. A., & Cate, J. H. D. (2005). Accessibility of 18S rRNA in human 40S subunits and 80S ribosomes at physiological magnesium ion concentrations—Implications for the study of ribosome dynamics. *RNA*, 11(12), 1898–1908. <https://doi.org/10.1261/rna.2192805>

Shigeoka, T., Koppers, M., Wong, H. H.-W., Lin, J. Q., Cagnetta, R., Dwivedy, A., de Freitas Nascimento, J., van Tartwijk, F. W., Ströhl, F., Cioni, J.-M., Schaeffer, J., Carrington, M., Kaminski, C. F., Jung, H., Harris, W. A., & Holt, C. E. (2019). On-Site Ribosome Remodeling by Locally Synthesized Ribosomal Proteins in Axons. *Cell Reports*, 29(11), 3605-3619.e10. <https://doi.org/10.1016/j.celrep.2019.11.025>

Stefani, G., Fraser, C. E., Darnell, J. C., & Darnell, R. B. (2004). Fragile X Mental Retardation Protein Is Associated with Translating Polyribosomes in Neuronal Cells. *Journal of Neuroscience*, 24(33), 7272–7276. <https://doi.org/10.1523/JNEUROSCI.2306-04.2004>

Steward, O., & Worley, P. F. (2001). Selective targeting of newly synthesized Arc mRNA to active synapses requires NMDA receptor activation. *Neuron*, 30(1), 227–240. [https://doi.org/10.1016/s0896-6273\(01\)00275-6](https://doi.org/10.1016/s0896-6273(01)00275-6)

Smith, P.R., Loerch, S., Kunder, N. *et al.* Functionally distinct roles for eEF2K in the control of ribosome availability and p-body abundance. *Nat Commun* **12**, 6789 (2021).

<https://doi.org/10.1038/s41467-021-27160-4>

Sossin, W. S., & DesGroseillers, L. (2006). Intracellular trafficking of RNA in neurons. *Traffic (Copenhagen, Denmark)*, *7*(12), 1581–1589. <https://doi.org/10.1111/j.1600-0854.2006.00500.x>

Sutton, M. A., Ito, H. T., Cressy, P., Kempf, C., Woo, J. C., & Schuman, E. M. (2006). Miniature Neurotransmission Stabilizes Synaptic Function via Tonic Suppression of Local Dendritic Protein Synthesis. *Cell*, *125*(4), 785–799. <https://doi.org/10.1016/j.cell.2006.03.040>

Sutton, M. A., Taylor, A. M., Ito, H. T., Pham, A., & Schuman, E. M. (2007). Postsynaptic Decoding of Neural Activity: eEF2 as a Biochemical Sensor Coupling Miniature Synaptic Transmission to Local Protein Synthesis. *Neuron*, *55*(4), 648–661.

<https://doi.org/10.1016/j.neuron.2007.07.030>

Takei, N., Inamura, N., Kawamura, M., Namba, H., Hara, K., Yonezawa, K., & Nawa, H. (2004). Brain-derived neurotrophic factor induces mammalian target of rapamycin-dependent local activation of translation machinery and protein synthesis in neuronal dendrites. *The Journal of Neuroscience: The Official Journal of the Society for Neuroscience*, *24*(44), 9760–9769.

<https://doi.org/10.1523/JNEUROSCI.1427-04.2004>

Tang, S. J., Reis, G., Kang, H., Gingras, A.-C., Sonenberg, N., & Schuman, E. M. (2002). A rapamycin-sensitive signaling pathway contributes to long-term synaptic plasticity in the hippocampus. *Proceedings of the National Academy of Sciences of the United States of America*, *99*(1), 467–472. <https://doi.org/10.1073/pnas.012605299>

Thoreen, C. C., Chantranupong, L., Keys, H. R., Wang, T., Gray, N. S., & Sabatini, D. M. (2012). A unifying model for mTORC1-mediated regulation of mRNA translation. *Nature*, *485*(7396), 109–113. <https://doi.org/10.1038/nature11083>

Tsang, B., Arsenault, J., Vernon, R. M., Lin, H., Sonenberg, N., Wang, L.-Y., Bah, A., & Forman-Kay, J. D. (2019). Phosphoregulated FMRP phase separation models activity-dependent translation through bidirectional control of mRNA granule formation. *Proceedings of the National Academy of Sciences*, *116*(10), 4218–4227.

<https://doi.org/10.1073/pnas.1814385116>

Wang, X., Li, W., Williams, M., Terada, N., Alessi, D. R., & Proud, C. G. (2001). Regulation of elongation factor 2 kinase by p90RSK1 and p70 S6 kinase. *The EMBO Journal*, *20*(16), 4370–4379. <https://doi.org/10.1093/emboj/20.16.4370>

Warner, J., Madden, M. J., & Darnell, J. E. (1963). The interaction of poliovirus RNA with *Escherichia coli* ribosomes. *Virology*, *19*(3), 393–399. [https://doi.org/10.1016/0042-6822\(63\)90079-5](https://doi.org/10.1016/0042-6822(63)90079-5)

- Warner, J. R., & Knopf, P. M. (2002). The discovery of polyribosomes. *Trends in Biochemical Sciences*, 27(7), 376–380. [https://doi.org/10.1016/S0968-0004\(02\)02126-6](https://doi.org/10.1016/S0968-0004(02)02126-6)
- Waung, M. W., Pfeiffer, B. E., Nosyreva, E. D., Ronesi, J. A., & Huber, K. M. (2008). Rapid Translation of Arc/Arg3.1 Selectively Mediates mGluR-Dependent LTD through Persistent Increases in AMPAR Endocytosis Rate. *Neuron*, 59(1), 84–97. <https://doi.org/10.1016/j.neuron.2008.05.014>
- Wells, D. G. (2006). RNA-Binding Proteins: A Lesson in Repression. *Journal of Neuroscience*, 26(27), 7135–7138. <https://doi.org/10.1523/JNEUROSCI.1795-06.2006>
- Wenzel, J., David, H., Pohle, W., Marx, I., & Matthies, H. (1975). Free and membrane-bound ribosomes and polysomes in hippocampal neurons during a learning experiment. *Brain Research*, 84(1), 99–109. [https://doi.org/10.1016/0006-8993\(75\)90803-3](https://doi.org/10.1016/0006-8993(75)90803-3)
- Wu, B., Eliscovich, C., Yoon, Y. J., & Singer, R. H. (2016). Translation dynamics of single mRNAs in live cells and neurons. *Science*, 352(6292), 1430–1435. <https://doi.org/10.1126/science.aaf1084>
- Wu, C. C.-C., Zinshteyn, B., Wehner, K. A., & Green, R. (2019). High-Resolution Ribosome Profiling Defines Discrete Ribosome Elongation States and Translational Regulation during Cellular Stress. *Molecular Cell*, 73(5), 959-970.e5. <https://doi.org/10.1016/j.molcel.2018.12.009>
- Wu, T., Hu, E., Xu, S., Chen, M., Guo, P., Dai, Z., Feng, T., Zhou, L., Tang, W., Zhan, L., Fu, X., Liu, S., Bo, X., & Yu, G. (2021). clusterProfiler 4.0: A universal enrichment tool for interpreting omics data. *Innovation (Cambridge (Mass.))*, 2(3), 100141. <https://doi.org/10.1016/j.xinn.2021.100141>
- Yao, Y., Kelly, M. T., Sajikumar, S., Serrano, P., Tian, D., Bergold, P. J., Frey, J. U., & Sacktor, T. C. (2008). PKM zeta maintains late long-term potentiation by N-ethylmaleimide-sensitive factor/GluR2-dependent trafficking of postsynaptic AMPA receptors. *The Journal of Neuroscience: The Official Journal of the Society for Neuroscience*, 28(31), 7820–7827. <https://doi.org/10.1523/JNEUROSCI.0223-08.2008>
- Ying, S.-W., Futter, M., Rosenblum, K., Webber, M. J., Hunt, S. P., Bliss, T. V. P., & Bramham, C. R. (2002). Brain-Derived Neurotrophic Factor Induces Long-Term Potentiation in Intact Adult Hippocampus: Requirement for ERK Activation Coupled to CREB and Upregulation of Arc Synthesis. *The Journal of Neuroscience*, 22(5), 1532–1540. <https://doi.org/10.1523/JNEUROSCI.22-05-01532.2002>
- Yu, T., Jiang, J., Yu, Q., Li, X., & Zeng, F. (2023). Structural Insights into the Distortion of the Ribosomal Small Subunit at Different Magnesium Concentrations. *Biomolecules*, 13(3), Article 3. <https://doi.org/10.3390/biom13030566>

Zhang, J., Hou, L., Klann, E., & Nelson, D. L. (2009). Altered Hippocampal Synaptic Plasticity in the Fmr1 Gene Family Knockout Mouse Models. *Journal of Neurophysiology*, *101*(5), 2572–2580. <https://doi.org/10.1152/jn.90558.2008>

Zhang, G., Xu, Y., Wang, X., Zhu, Y., Wang, L., Zhang, W., Wang, Y., Gao, Y., Wu, X., Cheng, Y., Sun, Q., & Chen, D. (2022). Dynamic FMR1 granule phase switch instructed by m6A modification contributes to maternal RNA decay. *Nature Communications*, *13*(1), 859. <https://doi.org/10.1038/s41467-022-28547-7>

Zhu, P. J., Huang, W., Kalikulov, D., Yoo, J. W., Placzek, A. N., Stoica, L., Zhou, H., Bell, J. C., Friedlander, M. J., Krnjević, K., Noebels, J. L., & Costa-Mattioli, M. (2011). Suppression of PKR Promotes Network Excitability and Enhanced Cognition by Interferon- $\gamma$ -Mediated Disinhibition. *Cell*, *147*(6), 1384–1396. <https://doi.org/10.1016/j.cell.2011.11.029>